

A NOVEL DUAL MODELING METHOD FOR CHARACTERIZING HUMAN
NERVE FIBER ACTIVATION

A Thesis
presented to
the Faculty of California Polytechnic State University,
San Luis Obispo

In Partial Fulfillment
of the Requirements for the Degree
Masters of Science in Biomedical Engineering

by
Frank Daniel Sugden
December 2014

© 2014
Frank Daniel Sugden
ALL RIGHTS RESERVED

COMMITTEE MEMBERSHIP

TITLE: A Novel Dual Modeling Method For Characterizing
Human Nerve Fiber Activation

AUTHOR: Frank Daniel Sugden

DATE SUBMITTED: December 2014

COMMITTEE CHAIR: Robert Szlavik, Ph.D.
Professor, Biomedical and General Engineering
California Polytechnic State University, San Luis Obispo

COMMITTEE MEMBER: David Clague, Ph.D.
Professor, Biomedical and General Engineering
California Polytechnic State University, San Luis Obispo

COMMITTEE MEMBER: Scott Hazelwood, Ph.D.
Professor, Biomedical and General Engineering
California Polytechnic State University, San Luis Obispo

ABSTRACT

A Novel Dual Modeling Method For Characterizing Human Nerve Fiber Activation

Frank Daniel Sugden

Presented in this work is the investigation and successful illustration of a coupled model of the human nerve fiber. SPICE netlist code was utilized to describe the electrical properties of the human nervous membrane in tandem with COMSOL Multiphysics, a finite element analysis software tool. The initial research concentrated on the utilization of the Hodgkin-Huxley electrical circuit representation of the nerve fiber membrane. Further development of the project identified the need for a linear circuit model that more closely resembled the McNeal linearization model augmented by the work of Szlavik which better facilitated the coupling of both SPICE and COMSOL programs. Related literature was investigated and applied to validate the model. This combination of analysis tools allowed for the presentation of a consistent model and revealed that a coupled model produced not only a qualitatively comparable, but also a quantitatively comparable result to studies presented in the literature. All potential profiles produced during the simulation were compared against the literature in order to meet the purpose of presenting an advanced computational model of human neural recruitment and excitation. It was demonstrated through this process that the correct usage of neuron models within a two dimensional conductive space did allow for the approximate modeling of human neural electrical characteristics.

Keywords: Myelinated neuron model, Equivalent circuit neuron model, Finite element model, Functional electrical simulation

TABLE OF CONTENTS

	Page
LIST OF TABLES	vii
LIST OF FIGURES	viii
CHAPTER	
1 Introduction.....	1
1.1 Neuron Anatomy	3
1.2 Neural Communication	6
1.3 Neuron Models	8
1.3.1 Hodgkin-Huxley Neural Model.....	9
1.3.2 Core Conductor Model	12
1.3.3 Linear Cable Theory.....	15
1.4 Solving Methods	21
1.5 Finite Element Analysis	24
1.5.1 COMSOL Multiphysics.....	27
1.6 Similar Work in Modeling Human Nerve Fiber Characteristics.....	28
1.7 Project Objective	32
2 Methods	34
2.1 Two Dimensional COMSOL Model	35
2.2 SPICE Netlist Neural Modeling	40
2.3 COMSOL to SPICE Coupling	46
2.4 Geometry Meshing.....	48
2.5 Simulation Solving.....	51
3 Results.....	53
3.1 Final Result Presentation.....	53
4 Discussion.....	58
4.1 Boundary Current Source.....	58
4.2 Voltage Source Inclusions.....	59
4.3 Membrane Potentials.....	61
4.4 Future Work	63

REFERENCES	65
APPENDICES	
Appendix A: Non-Linear SPICE Netlist Code	69
Appendix B: Linear SPICE Netlist Code	77
Appendix C: COMSOL Solver Log.....	85

LIST OF TABLES

Table		Page
1.	An assorted summary of the parameter variables, constants and expressions used in Szlavik's linear cable model adapted from McNeal's model and used to calculate the circuit network components. [37].....	20
2.	Dielectric properties of selected tissues at 433 MHz. [15].....	39
3.	Biologic membrane electrical characteristics of potassium ion channel values used in the SPICE neuron model presented as an example of the advanced functionality not allowed by COMSOL.....	44

LIST OF FIGURES

Figure	Page
1. Organizational levels of the human nervous system. [23].....	4
2. Three-dimensional view of a section of a nerve displaying connective tissues. [3].....	5
3. Visual representation of a nerve impulse propagation down the length of an axon due to ion exchange. [38].....	6
4. Hodgkin-Huxley electrical circuit representation of the nerve fiber membrane. [18].....	10
5. Electrical circuit network representing the core conductor model. [41].....	12
6. Cylindrical geometry of the core conductor model of a biological nerve fiber cell and the close examination of the membrane electrical characteristics. [41].....	14
7. McNeal representation of supposed myelinated nerve fiber electrical network model. [26].....	17
8. Szlavik equivalent circuit network for a myelinated nerve fiber superimposed on an axial cross section of a nerve fiber. [37].....	18
9. Example PSPICE circuit simulation schematic including values and labels for all components. [42].....	22
10. PSPICE netlist code example showing representations of various circuit elements including a current source, resistor and capacitor as taken from a portion of an iteration of this work.....	23
11. The first finite element mesh used in the work of Ari Adini under the direction of Ray Clough. [8].....	26
12. Graphical example of stress and strain concentrations in a finite element model of a wrench produced in COMSOL Multiphysics. [9].....	27
13. COMSOL simulation representing the human forearm in a NCV test created by Nathan Soto. [35].....	29

14.	PSPICE schematics representation of an equivalent circuit model of a human myelinated axon. [35].....	30
15.	SPICE HH model of a neuron producing a characteristic action potential as developed and implemented by Nathan Angel. [1].....	31
16.	Resultant intracellular and extracellular potential from the applied stimulus pulse as done in the coupled 1D muscle fiber in the 2D bulk volume conductor. [25].....	32
17.	Resultant COMSOL simulation product of SPICE netlist code incorporated into a segmented volume conductor in version 4.3.....	35
18.	Cut view representation of the human forearm used as a model for geometry development. [24].....	37
19.	Subdomain selection of the skin segments on top and bottom of the model and the small segment between the bone and ground electrode on the side to better simulate a natural occurring ground electrode.....	40
20.	Electrical current source statement written in SPICE code to be used with the included "Neuron_5" library.....	41
21.	a) Partial representation of robust HH model of human electrical neural characteristics as developed by Nathan Angel under the direction of Dr. Robert Szlavik. b) Linear netlist circuitry code partial representation of created model of human neural membrane electrical characteristics..... ..	43
22.	SPICE circuit netlist coding responsible for COMSOL nodal connections of voltage sources.....	46
23.	Piecewise continuous function created to serve as the pulse current source necessary for correct neural simulation.....	46
24.	Mesh convergence plot created in Microsoft Excel using data generated in COMSOL Multiphysics.....	50
25.	Mesh geometry of developed COMSOL simulation describing a cut view of a human forearm.....	51
26.	Boundary current source potential profile created from COMSOL..... ..	54
27.	COMSOL created voltage to ground measurements in the electric currents module translated to grounded voltage sources in the electric circuit module.....	55

28.	McNeal calculated solution for control comparison in simulation analysis. [26].....	56
29.	COMSOL generated human nerve membrane potential profiles.....	56
30.	Electric potential profile of the terminal boundary condition located directly below the current source.....	57

1 Introduction

The modern biomedical engineering field now encompasses a wide variety of cross disciplines requiring continued cooperation and exchange of information between many diverse groups including, but not limited to, the medical profession, academic projects and computer technology. Various current research projects focus on the use of biological tissue properties to optimize the placement of electrical systems like pacemakers [17]. Another important field of research is the need for mechanical analysis to be applied to modern technology in order to improve medical devices utilized for prosthetics that interact with the human nervous system. Part of that analysis requires a more precise representation of the electrical impulses of the human nerve fiber, which could greatly enhance the communication between the patients' nervous system and the articulation of the attached mechanical prosthetic [21]. Such a model could also impact a wide range of medical treatments besides neuroprosthetics. As an example, one current treatment for chronic pain relief includes the insertion of a pain relief device into a patient's back and spinal cord to target nerve bundles [33]. With the development of an advanced computational model, specific, individual nerve fibers, instead of nerve bundles, may eventually be targeted to relieve pain more effectively. The presentation of an advanced computational model of human neural recruitment and excitation is the focus of this work. This was accomplished by combining human neural characteristics with a selected computational model. The model is represented through circuit elements in conjunction with a software program designed to solve complex equations including the coupling of various elements such as water flow, electrical current transmission, and physical pressures.

The basis of this model began with the published research in 1952 in the Journal of Physiology, by Alan Lloyd Hodgkin and Andrew Huxley who developed a mathematical model of neural characteristics to aid in the understanding of action potential (AP) initiation and propagation in human nerves [18]. The Hodgkin-Huxley (HH) model uses circuit elements, both linear and non-linear, to model ion channel behavior in neurons. The differential equations they included in their presentation can be implemented with the circuit elements available in the Simulation Program with Integrated Circuit Emphasis (SPICE) model and the COMSOL Multiphysics model developed to computationally simulate electrical current and potential propagation in biologic tissues. These programs when coupled together targeted to produce a robust and powerful tool for modeling human neural activation potential initiations and propagations. However, even these advanced technologies have their own innate limitations. As it relates to this work, the non-linear characteristics of the HH model forced the redirection of the research, as well as the process and procedures necessary to properly investigate the activation of a nerve fiber. As a result, a simplified version of linear cable theory was developed within existing system requirements to allow for COMSOL coupling. In practice, the assumption that a human nerve fiber may be represented linearly is appropriate in computationally intensive simulations when the further assumption is presented that the conductance of the membrane is linear until excitation [26, 37]. With this assumption, the human myelinated nerve axon can be represented linearly using relatively simple circuit elements and thus properly represented in a coupled, interactive system with COMSOL Multiphysics.

COMSOL Multiphysics, as previously stated, is a robust multiphysics finite

element analysis tool developed originally by a number of graduate students at the Royal Institute of Technology in Stockholm Sweden, as a partial differential equation (PDE) toolbox for Matrix Laboratory (MATLAB). COMSOL has now been developed and specifically designed to become a multiphysics software tool capable of performing interactive simulations including but not limited to electrical propagation and fluid mechanics. Because of its design as a software program to be coupled with other systems, COMSOL has become a vital element in nerve fiber research.

To better understand the relevance and interaction of all these components, it is important to describe in more detail the individual components utilized in this project including the SPICE platform and COMSOL multiphysics software. It is also necessary to include an overview of neuron physiology and anatomy as well as a review of the development and methodology of existing mathematical models of nerve fibers.

1.1 Neuron Anatomy

The nervous system is a complex system responsible for every thought, action and emotion throughout the human body. This complex system is divided into multiple parts as seen in Figure 1. First is the central nervous system (CNS) which includes the brain and spinal cord. The CNS interprets sensory input and dictates motor responses. Next is the peripheral nervous system (PNS), composed mainly of the nerves that extend outward from the brain and spinal cord, including the nerves for motor function [24]. This system is further broken down into both the somatic nervous system and the autonomic nervous system (ANS), which includes sympathetic and parasympathetic nerve fibers [24]. This study focuses on the activation of nerves within the somatic nervous system.

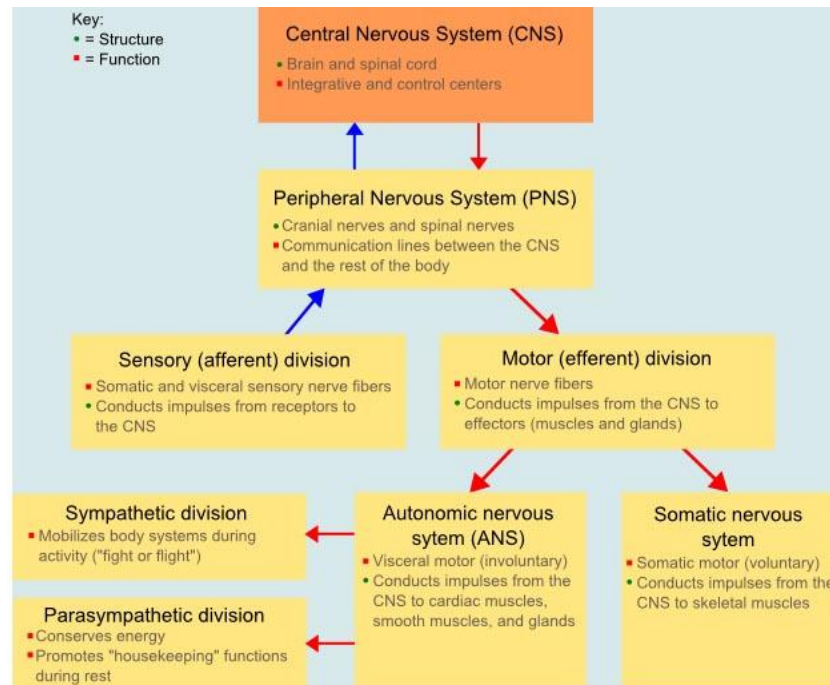


Figure 1: Organizational levels of the human nervous system. [23]

Within all divisions of the nervous system, the nerve cell, or neuron, is the structural unit responsible for impulse propagation and cellular communication. Most neuron cell bodies are present in the CNS with extensions outside the brain and spinal cord to reach the intended effector. These long extensions from the cell body of a neuron are referred to as axons. Any long axon that extends from the cell body of its neuron to reach its intended effector may also be referred to as a nerve fiber. Some long axons, or nerve fibers, can exceed three feet in length to reach their effector such as the motor neurons controlling the skeletal muscles of the big toe extending from the lumbar region in the spine to the bottom of the foot [24].

A multitude of axons are grouped together into structures known as fascicles. Fascicles are themselves grouped together into a nerve [24]. A nerve is the structure most easily visible to the human eye. Contained within the nerve and then within the fascicles are parallel bundles of peripheral axons enclosed by successive wrappings of connective

tissue known as the endoneurium [24]. Groups of fibers are then bound together inside the fascicle by a connective tissue known as the perineurium [24]. Finally all the fascicles and other various elements of a nerve are enclosed in a tough fibrous sheath known as the epineurium [24]. This entire grouping, as seen in Figure 2, is known as a nerve and is responsible for the transmission of biological signals. These signals are electrical impulses that travel down the length of an axon. Along its entire length, each axon is functionally considered the conducting region of the neuron responsible for transmitting nerve impulses [24].

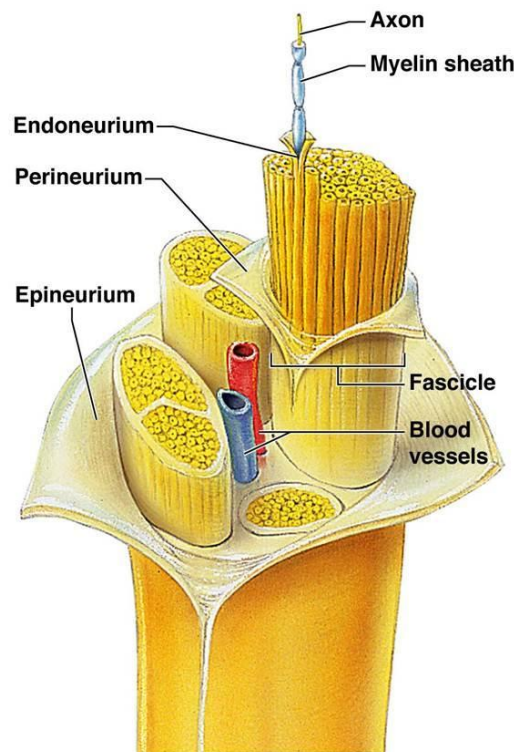


Figure 2: Three-dimensional view of a section of a nerve displaying connective tissues. [3]

The improved conduction properties of these Peripheral Nervous System (PNS) nerve fibers are due largely to the insulating myelin sheaths along the length of the nerve fiber created by Schwann cells. Schwann cells are unconnected fatty cells that attach and wrap around the nerve fiber in segments along its length to insulate the nerve fiber. As a

result, one fiber may have a multitude of Schwann cells attached with spaces in between as seen in Figure 3. This space or gap between Schwann cells is referred to as a node of Ranvier. It is at the nodes of Ranvier (NoR) where the impulses of a nerve fiber are re-generated through a series of ion exchanges, principally involving sodium and potassium.

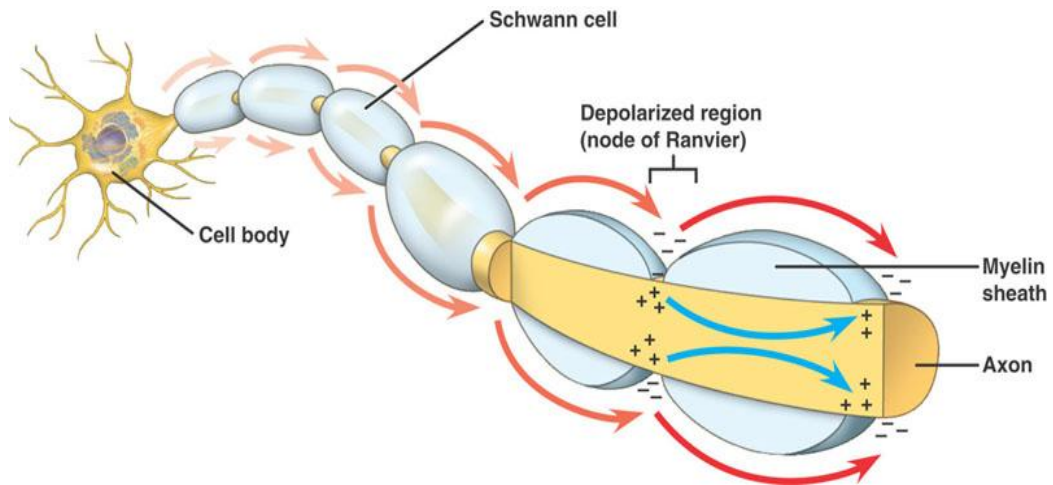


Figure 3: Visual representation of a nerve impulse propagation down the length of an axon due to ion exchange. [38]

1.2 Neural Communication

Ionic exchange of sodium and potassium ions accounts for the depolarization and subsequent repolarization of a nerve fiber. The exchange occurs across the cell plasma membrane and between the extracellular environment and the cell interior, or cytosol. A nerve fiber has a resting membrane potential of -70mV [24]. This is due to an interaction of ions and not due to an exchange of electrons as in most measurements of potential. Once enough sodium ions enter the cell, a threshold membrane potential between -55 and -50mV is reached and an impulse begins [24]. Potassium ions then leave the cell to repolarize the membrane potential. Influx and efflux of these ions results in a characteristic impulse referred to as an action potential (AP). This action potential is the impulse that is carried along the length of a nerve fiber and is responsible for the release

of neurotransmitters at the axon terminal that initiate some action. In essence, the action potential is the single most important characteristic of a nerve fiber as it is responsible for all the functions of a nerve.

An action potential cannot be initiated across a myelin sheath due to the insulating Schwann cells. Without access to extracellular ions, the portions of a nerve fiber encased in these Schwann cells are not capable of initiating an action potential but are capable of propagating one. Schwann cells not only keep outside ions from entering the nerve fiber, but the myelinated sheaths also keep ions from leaving the fiber. This means that the influx of charged ions at the node of Ranvier remains inside the fiber throughout the length of the Schwann cell and carries the charge along the axon. Charged ions enter the cell at a node of Ranvier and force membrane potentials above threshold which in turn causes an action potential that then propagates to the next node of Ranvier for the process to continue. This jumping of action potentials supports the fact that the conducting capabilities of PNS nerve fibers are due largely to Schwann cells.

Action potentials cannot be initiated directly next to each other because of the myelin sheaths surrounding most PNS nerve fibers and therefore must travel under the insulation of the Schwann cells to the next node of Ranvier where another action potential may be initiated. This type of conduction is referred to as saltatory conduction and is about 30 times faster than the type of conduction found along unmyelinated axons [24].

The exchange of ions at the nodes of Ranvier that produce this propagating action potential has been modeled along with the mathematical characteristics of a nerve fiber's excitation and propagation of an action potential. The myelinated section and nodes of

Ranvier along the length of a neuron may be modeled using linear circuit elements in an attempt to simplify the computational demands of modeling neural activity, which will be addressed in more detail.

1.3 Neuron Models

Beginning in the 1950's with the HH quantitative model of membrane current, the excitable properties of nervous conduction have been modeled various ways, including both linear and non-linear methods [18]. The HH solution presented fully in 1952 is a non-linear model based on extensive mathematical modeling that has been translated into an equivalent circuit that is representative of the membrane [18]. In 1968, Goldman and Albus presented a linear relationship between the conduction velocity of an action potential and the fiber diameter of the chosen nerve fiber using the work of Offner et.al. as a starting point [16, 30]. This was a linear simplification developed by utilizing equations that were previously derived empirically assuming point stimulation of an electrical impulse [16]. These models were valid, but the accurate representation of a real world stimulus required the introduction of a macroelectrode into the simulation [16]. Rushton and Lussier, in 1952, began the work of modeling neural threshold for a specific electrode geometry and continued to pursue this work to obtain an analytical solution for threshold based upon bipolar electrodes [22, 31]. Adding to the work of his predecessors, McNeal attempted to present a model describing the electrical properties of myelinated nerve fibers using arbitrary electrode configurations which incorporated the efforts of these previous studies [26].

All these studies attempted to present a theoretical model for nervous conduction; all included different assumptions; all were idealizations of the physiology and all

required further development from the original presentation. The study presented in this thesis originally chose the HH neural model as the most representative mathematical model of human nervous conduction.

1.3.1 Hodgkin-Huxley Neural Model

In the HH model, Hodgkin and Huxley proposed that the electrical behavior of the nerve fiber membrane could be represented by the circuit network shown in Figure 4. Their model suggested that the current across the membrane could be transmitted by charging the membrane capacitance, represented by a capacitor, or by the movement of ions through the parallel resistances [18]. This movement of ions could be considered the basis of the HH model, as it is the charged ions that are responsible for the membrane potential. As previously discussed, the ions involved are mainly sodium and potassium, which are both positively charged ions. The translation of sodium ions into the cell across the cell membrane is responsible for the quick depolarization of the membrane while the slower translation of potassium ions out of the cell across the membrane is responsible for the repolarization of the membrane. Other ions are involved such as chloride and, in cardiac cells, calcium, but it is sodium and potassium that Hodgkin and Huxley chose to focus on. The final ionic current illustrated in the circuit diagram, I_L , is referred to as the "leakage current" and it represents a membrane current composed of chloride and other ions [18].

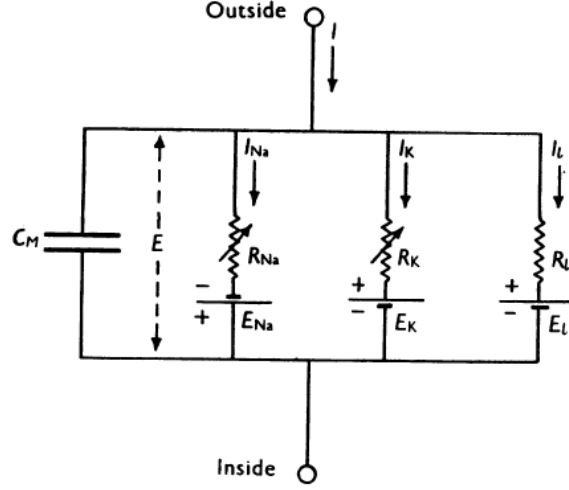


Figure 4: Hodgkin-Huxley electrical circuit representation of the nerve fiber membrane. [18]

Other circuit elements included in the presentation also serve a purpose when it comes to modeling the electrical behavior of the membrane. The values R_{Na} , R_K , and R_L are more commonly represented as conductances, or inverse resistances, and are useful in determining their applicable ionic currents since the difference in potential multiplied by the conductance produces a current. Ohm's law,

$$V = IR \quad (1)$$

which can be manipulated to

$$I = V * \frac{1}{R} = VG \quad (2)$$

where G represents a conductance, is applied at this juncture since it states that the current through a conductor between two points is directly proportional to the potential difference across the two points [18]. E_{Na} , E_K , and E_L represent equilibrium potentials for their respective ions. Calculating the ionic current through each respective channel required taking the difference between the membrane potential, E , and the ionic equilibrium potential to produce the potential difference, or voltage [18]. Hodgkin and Huxley experimentally discovered that the conductances G_{Na} and G_K are non-linear

functions of time and membrane potential, making the HH model a non-linear model that describes membrane electrical behavior.

Describing membrane electrical behavior for nerve fibers using a mathematical model requires using a system of equations to represent the initiation and propagation of the action potential. Hodgkin and Huxley produced the following to describe the potassium conductance

$$G_K = \overline{G_K} n^4 \quad (3)$$

$$\frac{dn}{dt} = \alpha_n(1 - n) - \beta_n n \quad (4)$$

where $\overline{G_K}$ is a constant, α_n and β_n are rate constants that vary with membrane potential, and n is a dimensionless variable that varies between zero and one [18]. Through a similar process, the following was derived to represent the sodium conductance

$$G_{Na} = \overline{G_{Na}} m^3 h \quad (5)$$

$$\frac{dm}{dt} = \alpha_m(1 - m) - \beta_m m \quad (6)$$

$$\frac{dh}{dt} = \alpha_h(1 - h) - \beta_h h \quad (7)$$

where n , m and h represent dimensionless variables that vary between zero and one [18]. Also $\overline{G_{Na}}$ is similar to $\overline{G_K}$ in that both are constants and represent the maximal sodium and potassium conductances [18]. Assuming that the voltage is the same everywhere inside the cell, this method is valid. For an electrically large cell where the potential is not the same everywhere inside the cell the HH model fails as it does not account for spatial variation of potential.

1.3.2 Core Conductor Model

To account for this lack of spatial variability, the core conductor model must be used. Originally derived as a partial differential equation (PDE) by Hermann and Weber in the 1870s, the core conductor model is a solution to electric current flow in and around a nerve fiber model accounting for spatial variation [20]. The PDEs originally developed have since been translated into electrical circuit elements and are most commonly seen as in Figure 5 below. The original PDEs are represented as circuit elements that can account for spatial differences through the representation of variable conductances and currents across a represented nerve fiber membrane and not through the representation of ion channels as in the HH model [41]. The core conductor model's variable conductances and currents represent an abstraction from the biologic nerve fiber and use a cylindrical cell geometry as opposed to the work of HH [41]. This model of cylindrical geometry uses variable currents to closely represent the electrical characteristics of a biologic nerve fiber [41].

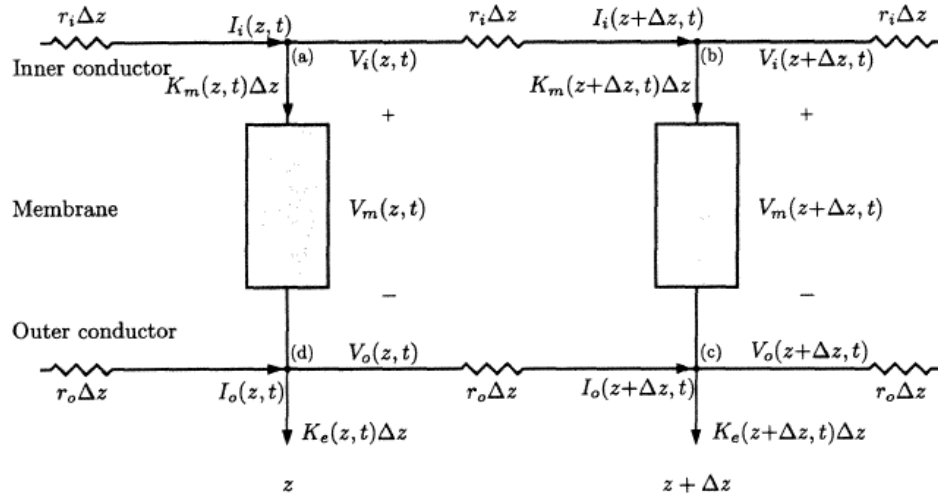


Figure 5: Electrical circuit network representing the core conductor model. [41]

In order to use this model as an accurate representation of the electrical characteristics of a biologic nerve fiber, there are some assumptions that must be made:

1. The membrane is cylindrical in geometry and separates two homogenous and isotropic conductors of electric current that obey Ohm's Law (1), i.e. the intracellular and extracellular space [41].
2. All the electrical characteristic variables are independent of angle and therefore have cylindrical symmetry [41].
3. Because the quasi-static terms of Maxwell's equations are sufficient and electromagnetic radiation effects are negligible, a circuit theory approach is adequate to describe the of currents and voltages [41].
4. The direction of currents are identical according to their respective locations in that currents in the conductors flow longitudinally and currents in the membrane flow radially only [41].
5. At any given point along the cell, the inner and outer conductances must be equipotential, so that the only difference is in the radial direction across the membrane [41].

With these assumptions in place, the core conductor model may be used to approximate the electrical characteristics of a nerve fiber. The I_o and I_i variables in Figure 6 represent longitudinal currents in their respective conductors [41]. J_m represents membrane current density whereas K_m represents membrane current per unit length [41]. V_m , V_i , and V_o represent membrane and conductor potentials [41]. Resistances in the conductors are represented by r_i and r_o and the radius of the cylindrical cell is

represented by a [41]. Finally K_e represents the current per length due to external sources [41].

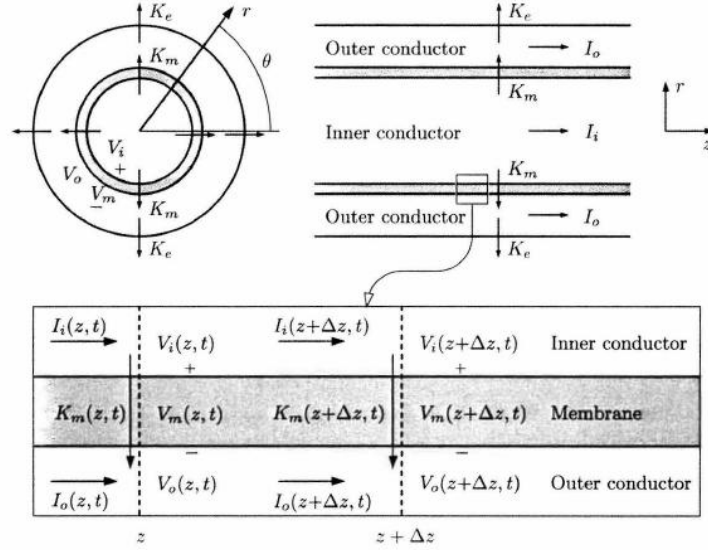


Figure 6: Cylindrical geometry of the core conductor model of a biological nerve fiber cell and the close examination of the membrane electrical characteristics. [41]

Through the use of Kirchoff's current law (KCL) and various circuit theory laws, the above variables can be used to represent the changing membrane voltage. Initially, describing the nodal currents through the use of KCL equations yields a system of equations describing applied currents within the cylindrical model. Using the voltage drop across a resistor yields an equation describing a change in potential. Applying Kirchoff's voltage law (KVL) provides a system of equations for loop voltages. Finally, by taking partial derivatives and after some algebra, what is sometimes referred to as the core conductor equation may be derived as seen below [41].

$$\frac{\partial^2 V_m(z, t)}{\partial z^2} = (r_0 + r_i)K_m(z, t) - r_o K_e(z, t) \quad (8)$$

As can be seen from equation (8), the core conductor model accounts for spatial variability in electrical potential within the cell. The issue of representing spatial

variability can be most easily seen in Figure 5 where there is an evident lack of electrical membrane characteristics specifically and only a circuit representation of the cylindrical fiber conductors. When these laws and equations are applied to the HH model already reviewed, the solution becomes more evident. The HH model specifically describes the electrical characteristics of the membrane but lacks spatial variability and the core conductor model describes spatial variability but lacks specific membrane electrical characteristics. The two are combined to create a non-linear representation of the nerve fiber describing specific membrane characteristics as well as accounting for spatial variability. This combination was the original choice for modeling the electrical characteristics of a nerve fiber in this work.

1.3.3 Linear Cable Theory

As much as the above combination of the HH model and core conductor model make logical sense as the required basis of this work, software restrictions related to communication between COMSOL and SPICE required deviation from this combination if the project was to proceed successfully. COMSOL is software capable of incorporating circuit networks into finite element analysis but, as it is not designed specifically for use in circuitry analysis, there are specific restrictions as described below that make the incorporation of non-linear elements in the advanced model no longer a viable option. Further analysis revealed that the implementation of a simplified linear cable theory was necessary to assure progress and thus it became the ultimate component to be included in this work.

In 1855 Professor William Thomson, later Lord Kelvin, derived and applied the PDE cable equation,

$$\lambda^2 \left(\frac{\partial^2 V}{\partial x^2} \right) - V - \tau \left(\frac{\partial V}{\partial t} \right) = 0 \quad (9)$$

or, in terms of the dimensionless variables, $X = \frac{x}{\lambda}$ and $T = \frac{t}{\tau}$

$$\left(\frac{\partial^2 V}{\partial X^2} \right) - V - \left(\frac{\partial V}{\partial T} \right) = 0 \quad (10)$$

to calculations essential for the first transatlantic telegraph cable. Thus the designation "cable theory" was created [20]. Thomson knew that the cable equation PDE was formally the same PDE Fourier used to describe the conduction of heat in a wire or ring [20]. Hermann and Weber had devised a separate PDE recognized as the core conductor equation as seen above, which for use in linear cable theory must be reduced to one spatial dimension [20]. Rewriting the cable equation as

$$\left(\frac{\partial^2 V}{\partial X^2} \right) = V + \left(\frac{\partial V}{\partial T} \right) \quad (11)$$

it can more easily be seen, as Hermann and others recognized, that the one dimensional presentation of the core conductor equation is in fact Kelvin's cable equation [20]. This mathematical representation of the linear cable theory was experimentally tested with single-fiber preparations in the 1930s and provided evidence to confirm the relevance of cable theory in representing nerve fibers [20].

Nerve axons or fibers have since been represented using the linear cable theory many times with expansions and further derivations conducted. One such expansion on the original linear cable theory and also cited and used in Szlavik's work [37] is the publication of McNeal [26]. McNeal presented the circuit network in Figure 7 as an advanced form of the linear cable theory including fiber diameter dependent variables [26]. He later included a table of variables and constants to be used in the derivation of

the defining expressions for his linear cable model [26]. The derivations begin by defining expressions for the internodal conductance

$$G_a = \frac{\pi d^2}{4\rho_i L} \quad (12)$$

and the capacitance and conductance portions of the membrane impedance,

$$C_m = c_m \pi d l \quad (13)$$

and

$$G_m = g_m \pi d l \quad (14)$$

respectively [26]. The constant V_r was expressed as $-70mV$ and represents the resting membrane potential [26]. V_e and I_n are external nodal voltages and membrane currents at their respective nodes [26]. Through examination of the characteristic expressions for McNeal's model

$$C_m \frac{dV_n}{dt} + I_{i,n} = G_a (V_{i,n-1} - 2V_{i,n} + V_{i,n+1}) \quad (15)$$

and the constants and variables, it can be easily seen that the proposed model is a solution that is time, voltage, and space dependent [26].

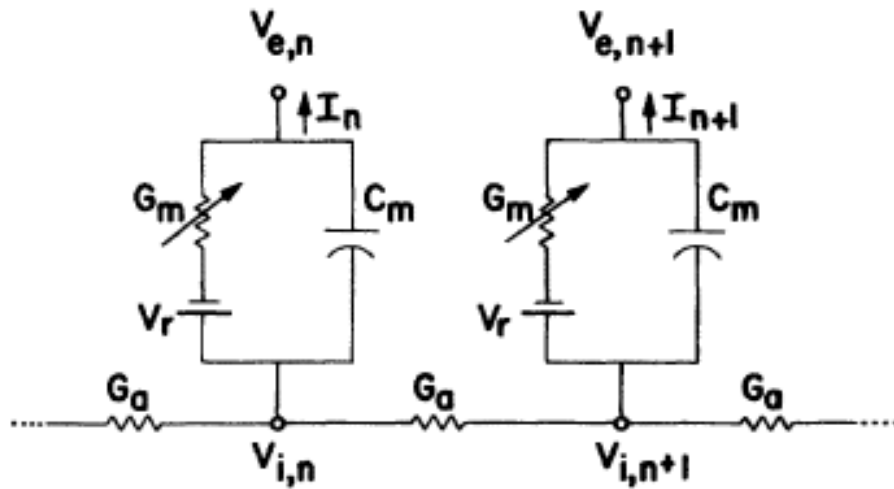


Figure 7: McNeal representation of supposed myelinated nerve fiber electrical network model. [26]

Szlavik adapted this model to include inverse conductances, or resistances, along the fiber as part of the contribution to membrane impedance, in addition to providing a more relatable representation of external stimulation as illustrated by the V_e sources above [37]. This revised model, as seen in Figure 8, was selected for use in this work.

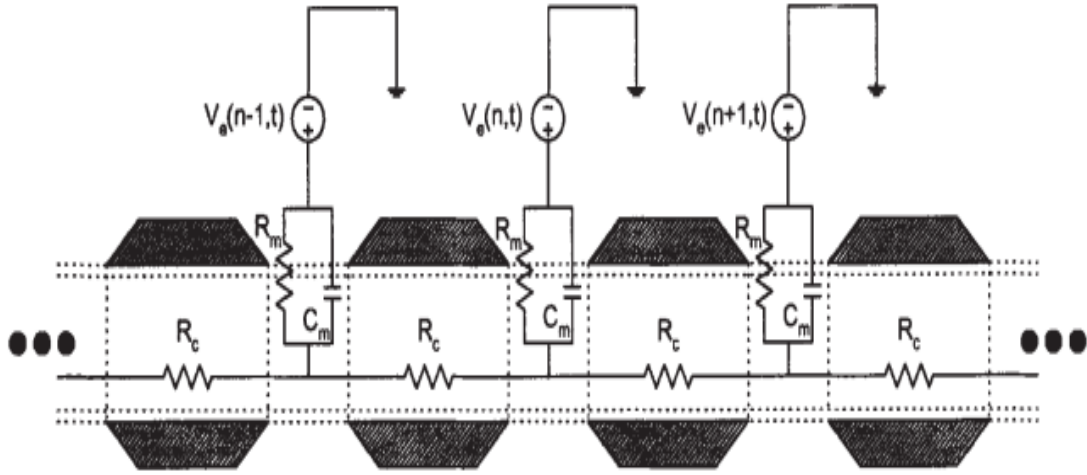


Figure 8: Szlavik equivalent circuit network for a myelinated nerve fiber superimposed on an axial cross section of a nerve fiber. [37]

Applying KCL at the intracellular nodes, a differential equation describing the circuit network characteristic expression was derived by Szlavik as

$$\begin{aligned}
 C_m \frac{dV_m(n, t)}{dt} + G_m V_m(n, t) \\
 &= G_c (V_m(n-1, t) - 2V_m(n, t) + V_m(n+1, t)) \quad (16) \\
 &+ V_e(n-1, t) - 2V_e(n, t) + V_e(n+1, t)
 \end{aligned}$$

when re-arranged to place like terms on the same side of the equal sign [37]. This characteristic equation representing the linear cable theory network is very similar to the work presented by McNeal above considering that conductance, G , is inverse resistance and so

$$G = \frac{1}{R} \quad (17)$$

where R stands for resistance. Because of the relationship between conductance and resistance, Ohm's Law in equation (2) may be used to demonstrate that Szlavik's equation can be re-written to more closely resemble McNeal's work in that

$$\begin{aligned} C_m \frac{dV_m(n, t)}{dt} + I_m(n, t) \\ = G_c(V_m(n-1, t) - 2V_m(n, t) + V_m(n+1, t)) \\ + V_e(n-1, t) - 2V_e(n, t) + V_e(n+1, t)) \end{aligned} \quad (18)$$

where

$$V_m = V_i - V_e - V_t \quad (19)$$

at each node and V_i is the resting membrane potential [37]. With the use of the expression for transmembrane potential V_m and the knowledge that V_i is a constant, Szlavik's derivation is nearly identical to McNeal's work in representing the electrical behavior of a human nerve fiber using linear electrical networks.

Because of this similarity, Szlavik attached the summary in Table 1 of variables, constants and expressions based on McNeal's presented work [37]. The expressions presented for fiber and axon radius were not originally present in Szlavik's table but have since been added as a simple relationship to their respective diameters. A value for fiber diameter was also not present in the original table but has since been added, taken from another publication to aid in the calculation of the circuit components [36]. This linear cable theory model used the ratio presented in the table below

$$\frac{d}{2} = 0.7 \frac{D}{2} \quad (20)$$

to determine the value for axon diameter so that the only value added to the original table was fiber diameter, as discussed above.

Table 1: An assorted summary of the parameter variables, constants and expressions used in Szlavik's linear cable model adapted from McNeal's model and used to calculate the circuit network components. [37]

ρ_a	Cytoplasm resistivity	1.1 (Ωm)
g_m	Membrane conductance	304 (S/m^2)
c_m	Membrane capacitance	0.02 (F/m^2)
l	Node of Ranvier width	2.5 (μm)
D	Fiber diameter	1.2E-5 (m)
d	Axon diameter	8.4E-6 (m)
A	Fiber radius	$D/2$ (m)
a	Axon radius	$d/2$ (m)
a/A	Ratio of axon to fiber radius	0.7
K	Nodes of Ranvier spacing	$100 * D$ (m)
R_c	Equivalent axoplasm resistance	$(\rho_a K)/(\pi a^2)$ (Ω)
R_m	Equivalent membrane resistance	$(2\pi g_m a l)^{-1}$ (Ω)
C_m	Equivalent membrane capacitance	$(2\pi c_m a l)$ (F)

To use this linear cable model of human nerve fiber excitation using circuit elements along with the inherent variables, constants and expressions requires some assumptions. Because of its similarity to McNeal's work, certain assumptions presented by McNeal also apply to the model proposed by Szlavik:

1. The myelin sheath is a perfect insulator.
2. The fiber consists of regularly spaced nodes of Ranvier.
3. The internodal distance is proportional to fiber diameter.
4. There exists a constant nodal gap width, which suggests that the nodal membrane area is also proportional to fiber diameter [26].

5. The use of the model must assume that the electrical potential outside the fiber is not distorted by the presence of the fiber and thus is determined only by the stimulus, surrounding tissue and electrode geometry [26].
6. Negligible effects of the fiber on the external electrical potential is valid due to the small dimensions of a fiber [26].
7. The nodal voltage of the membrane's external surface is equipotential, so variations in membrane current density can be neglected [26].
8. Conductance of the membrane is linear until the point of nerve fiber excitation, where the internally generated currents become significant [37, 26].

1.4 Solving Methods

SPICE was chosen as the aforementioned circuit solver to compute a solution to the simplified linear cable theory network presented by Szlavik. First developed at the University of California, Berkeley by Nagel and Pederson in the Department of Electrical Engineering and Computer Sciences at the Electronics Research Laboratory in 1973, SPICE is a circuit simulation software package capable of creating and solving circuit problems using nodal analysis [29]. Since its original development, many software packages have successfully integrated SPICE into their platforms when circuit analysis has been a primary requirement. The two available SPICE platforms developed for this purpose were Linear Technology SPICE (LTSPICE) and Personal SPICE (PSPICE). PSPICE was the first SPICE version to become available for personal computer (PC) usage. Due to the demands of a broad user base the program has been continually upgraded to make it more user friendly. However, it restricts student users to a maximum of ten transistors in a single circuit model, thereby limiting its applicability for more complex projects. LTSPICE has no inherent circuit size restrictions but requires more robust computing power as compared to

PSPICE. Due to immediate availability and user training, PSPICE was the chosen tool for this work but PSPICE cannot stand alone in providing the simulation of a model for electrical propagation. This situation required the introduction of a different program, COMSOL, that does not deal mainly with circuitry but can be combined with SPICE elements and commands.

Providing a visual schematic of the SPICE software components as seen in Figure 9 is the first step toward understanding how the two programs can be merged. But a circuit schematic is just a visual representation of various circuit elements chosen by the user in an attempt to realize the real world application. SPICE solves circuits using a differential equation representation of circuit elements at all nodes. This is how SPICE was originally designed, as a nonlinear differential equation solver and it is how the various versions function today.

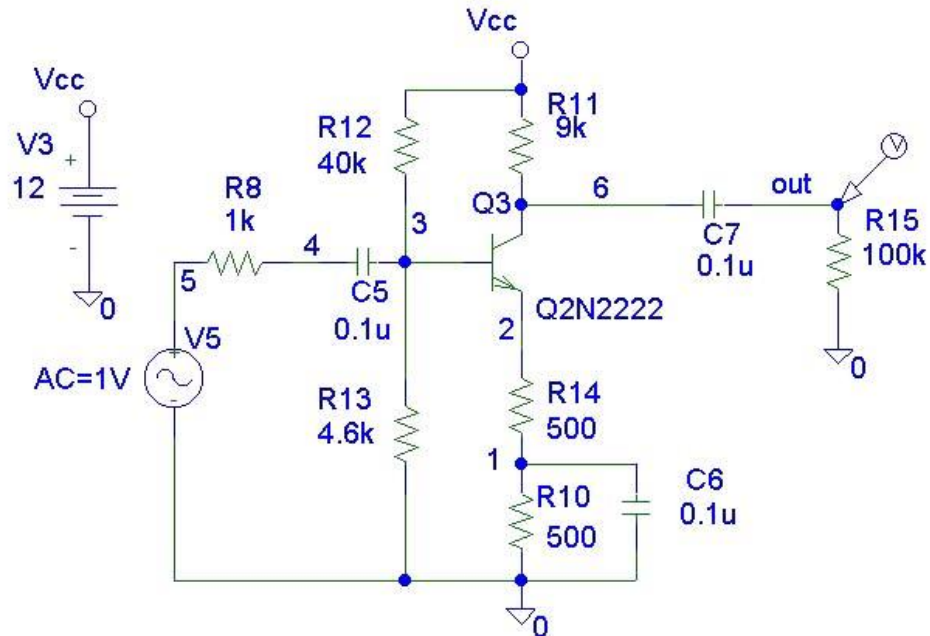


Figure 9: Example PSPICE circuit simulation schematic including values and labels for all components. [42]

SPICE solves circuits using netlist code as a representation of the devised circuit network and all its components. An example of PSPICE netlist code is presented in Figure 10, specifically a portion of an iteration of the code used in this work. As can be seen, netlist code uses a text-based format to represent elements in the form of letter variables with values. In essence, SPICE netlist code is a coding language for representing circuit elements. This is the basis of SPICE functionality as originally presented in the memorandum by Nagel and Pederson in 1973 [29]. Circuit analysis performed in this way allows for robust evaluation of networks through analysis commands implemented to perform various operations like transient analysis using ".TRAN" or Fourier analysis using ".FOUR" as two examples. Netlist code also provides a common method of specifying a circuit across platforms because it is the basic language of SPICE simulation software.

```
* Node of Ranvier Spacing (m)
.PARAM NODESPACE={100*FIBERDIA}
* Equivalent Axoplasm Resistance (ohm)
.PARAM EAXORES={ (CYTORES*NODESPACE)/(3.14159265359*(AXONRADIUS^2)) }
* Equivalent Membrane Resistance (ohm)
.PARAM EMEMRES={1/(2*3.14159265359*MEMCOND*AXONRADIUS*NODEWIDTH)}
* Equivalent Membrane Capacitance (F)
.PARAM EMEMCAP={ (2*3.14159265359*MEMCAP*AXONRADIUS*NODEWIDTH)}
* Calculation of Controlled Sources Gain Done in Accompanying Excel

*Connecting COMSOL nodes into circuit
X1 101 102 103 104 105 200 0 CONNECTIONS

*Current Source for COMSOL Simulation
I20 0 200 pulse(0 0.015 0.002 0.0000001 0.0000001 0.001 0.002)
*I + - pulse(initialcurrent pulsedcurrent delay falltime risetime pulsewidth period)

*Beginning Resistance Representing Myelinated Axoplasm
RBM 0 1 1867417999

*Node of Ranvier 1
G1 0 1 101 0 0.000231132075475 ;Intracellularly Injected Current Source Connections from COMSOL
R1 1 0 290853.3317 ;Membrane Resistance
C1 1 0 0.000000000226194671 ;Membrane Capacitance
```

Figure 10: PSPICE netlist code example showing representations of various circuit elements including a current source, resistor and capacitor as taken from a portion of an iteration of this work.

1.5 Finite Element Analysis

Communication between platforms using the SPICE netlist language to model and solve electrical networks is the basis of this work. The specific chosen software to be used as the modeling platform for this work in conjunction with a PSPICE circuit simulator was COMSOL Multiphysics. COMSOL Multiphysics is a finite element analysis tool used in a variety of dimensional problems across a broad array of fields including fluid dynamics, heating simulations, and electrical signal propagation evaluations. This aspect of finite element analysis was of primary importance when a tool was chosen to perform the evaluation in this work because of FEA's strong capabilities in modeling dimensional problems. Finite element analysis is a tool developed and used in a variety of applications to compute solutions to dimensional problems by dividing the presented geometries into many small, finite parts, or elements, and solves each element using different tools for analysis. The finite element method can be described as a numerical analysis technique used to compute approximate solutions to the presented problems [19]. Because the geometry is dissected into a finite number of small elements and each element is solved individually using the governing equations, the result is an approximate solution to the proposed problem and not an exact solution. An approximate solution is acceptable in that it is a reasonable representation of a real world physics problem solved using mathematically accurate governing equations. Real world problems also present the obstacle of complex geometries that would be computationally inhibitive to finding exact analytical solutions [19]. A physical problem of complex geometry can be approximately solved using an FEA tool like COMSOL multiphysics through the aid of dissecting these complex geometries into a finite number of manageable shapes that

carry the same physical principles and properties of their parent geometry. Once the physical principles and properties of initial conditions and boundary conditions are applied, the mathematical governing equations can be accurately solved.

COMSOL multiphysics is one of many FEA tools in use today. Originally the label "finite element method" was first used in a paper by Clough in 1960 [8]. Clough began with research in 1957 on computer analysis of structures [7]. Working with computer groups on the University of California Berkley's campus, Clough developed a matrix algebra program that could be used in conjunction with tape storage to solve more than 40 equations on the IBM 701 digital computer on campus [7]. Graduate student Ari Adini, under the direction of Clough, used the developed program and hand analysis of matrices to calculate and solve coarse mesh problems of plane stresses in continuous structures [7]. An example of Ari Adini's work is shown in Figure 11. Another graduate student under the direction of Clough was Ed Wilson, who hoped to decrease the large amount of work required to solve Adini's finite element problem. As a result, Wilson developed an automated finite element program based on the rectangular plane stress finite element method developed at Boeing [7]. The work of Ed Wilson was the first iteration of an FEA computational program to be used on a computer system. Control Data Corporation sold the first commercial finite element software in 1964 using a keypunched IBM card to represent each element and each node which engineers were forced to prepare node by node due to the lack of availability of mesh generators [19]. Since the introduction of workstations in 1980 and the development of personal computers, finite element software has progressed into an extremely cost effective problem solving option [19].

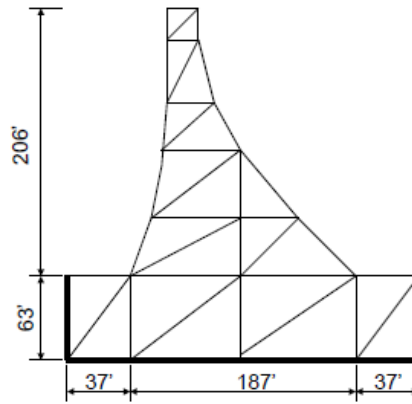


Figure 11: The first finite element mesh used in the work of Ari Adini under the direction of Ray Clough. [8]

Each of the cost effective finite element problem solving options as reviewed operate in a similar manner. In a continuum problem of any of the three dimensions, the field variable possesses a great number of possible values due to the position dependant variability of the general equations [19]. Finite discretization procedures performed in the chosen FEA software reduce the large number of variables in the problem to a finite amount by first dividing the provided geometry into a finite number of elements and then expressing the unknown field variable in terms of approximating governing equations within each element [19]. Nodes are thus created on the element boundaries where adjacent elements are connected with few interior nodes existing. It is at these nodes where the field variable is defined and the approximating functions solved [19].

Adjusting the size and number of these elements yields more or less accurate representations of real world situations; however, the solution is never fully accurate and is always an approximation. Governing equations are applied to each element, as described above, in order to formulate a solution to the whole dimensional problem. Solving the chosen equations for the field variable yields a number of results that, when combined, form the approximate solution to the proposed problem. With the finite

elements created and governing equations applied, the problem must be more accurately defined. Boundary and initial conditions are thus applied to the finite element model to aid in solving the systems of equations. Finally, a solving system must be selected that computes the most accurate solution to the complex problem. Such solvers include time dependent, stationary, and iterative solvers. Once compiled and solved, modern FEA software graphically presents a solution as seen in Figure 12.



Figure 12: Graphical example of stress and strain concentrations in a finite element model of a wrench produced in COMSOL Multiphysics. [9]

1.5.1 COMSOL Multiphysics

One such finite difference software package is COMSOL multiphysics. As discussed above, COMSOL originated as a PDE toolbox for MATLAB based on coding that a Swedish mathematician and numerical analyst from the Royal Institute of Technology in Stockholm developed that was originally entitled Femlab [34]. Today the COMSOL company has grown from Sweden to include offices in Brazil, China, Denmark, Finland, France, the U.S.A, and many more countries across the world [9]. Femlab is now COMSOL Multiphysics and is a finite element analysis tool used to model and simulate real world multiphysics systems through its many modules. Some examples

of the modules available for use in COMSOL multiphysics include structural mechanics, high and low frequency electromagnetics, fluid flow, and heat transfer [9]. Recently COMSOL added the feature of LiveLink to their product for computer aided design (CAD) software connectability to better aid their users in developing robust and complex three dimensional geometries for use in finite element analysis [9]. Finally COMSOL multiphysics is entitled as such due to its applicability to multiple physics simulations through the use of its physics modules. This multiphysics functionality allows COMSOL to be used as an advanced iterative solver of complex differential equations describing a wide variety of physical phenomena. An example of such iterative solving capability is the phenomena of joule heating resultant from an electrical current stimulus through a simulated resistive electrical impedance in a circuit. In COMSOL this could be considered three separate physics modules coupled to include joule heating, from electric currents, in an electric circuit. The setup would include creating an electric circuit to include a resistive impedance, forming a geometry to represent such an impedance, applying the three physics modules, defining subdomain and boundary conditions across all portions of the geometry, selecting a solver, and finally correctly visualizing the result.

1.6 Similar Work in Modeling Human Nerve Fiber Characteristics

A previous study related to the work of this thesis involved performing finite element analysis using the COMSOL software [35]. The work of Nathan Soto presented a bulk tissue representation of a human forearm to simulate a nerve conduction velocity (NCV) test in COMSOL as seen in Figure 13 [35]. Soto worked under the assumption that the human forearm could be modeled using a homogeneous, isotropic volume conductor as shown above with the exception of the modeled stimulating medical

electrode of normalized current density equal to 10A/m^2 [35]. Next in Soto's work, an equivalent circuit model of a myelinated axon was implemented in PSPICE schematics software using voltage values gathered from the COMSOL simulation as DC voltage sources as illustrated in Figure 14. The parallel resistor-capacitor (RC) network represents the nervous membrane and the remaining resistors represent the axoplasm resistance [37]. The simulation yielded DC voltage results for membrane potential without any RC characteristic response as may be expected over the course of two milliseconds [35]. Soto's work used a bulk media to extrapolate DC voltages which were entered into a simple SPICE simulation, but this work attempts to more accurately represent the human nerve fiber characteristics by parsing the bulk media.

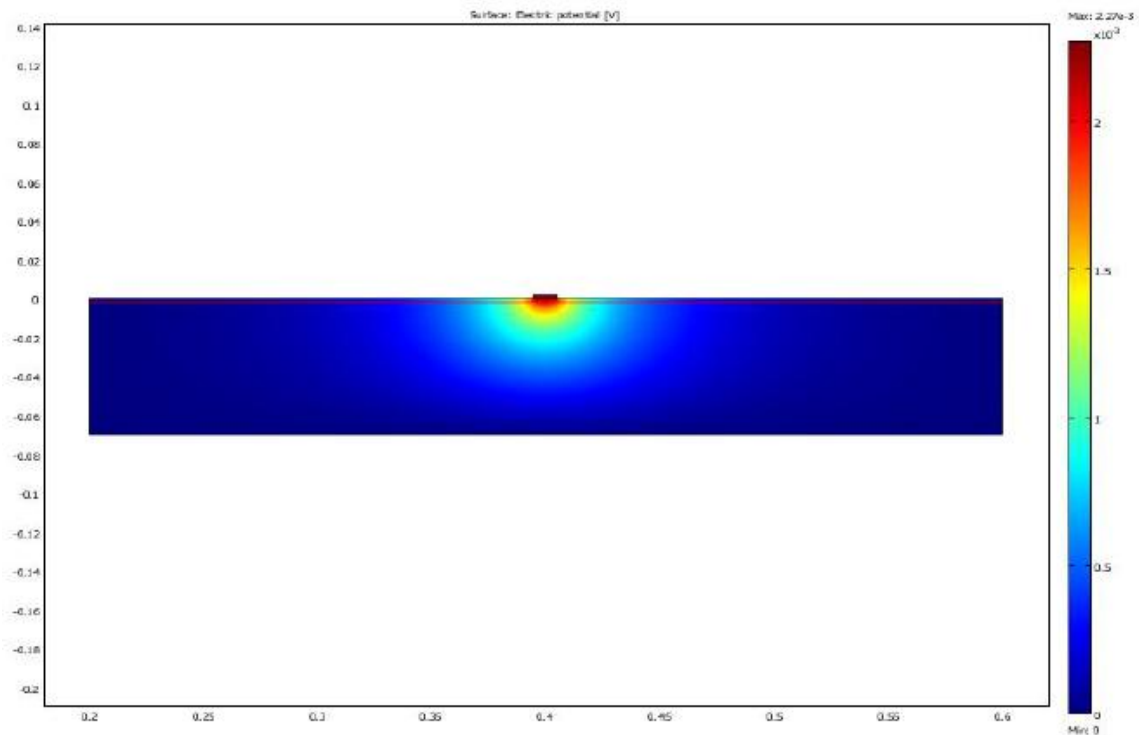


Figure 13: COMSOL simulation representing the human forearm in a NCV test created by Nathan Soto. [35]

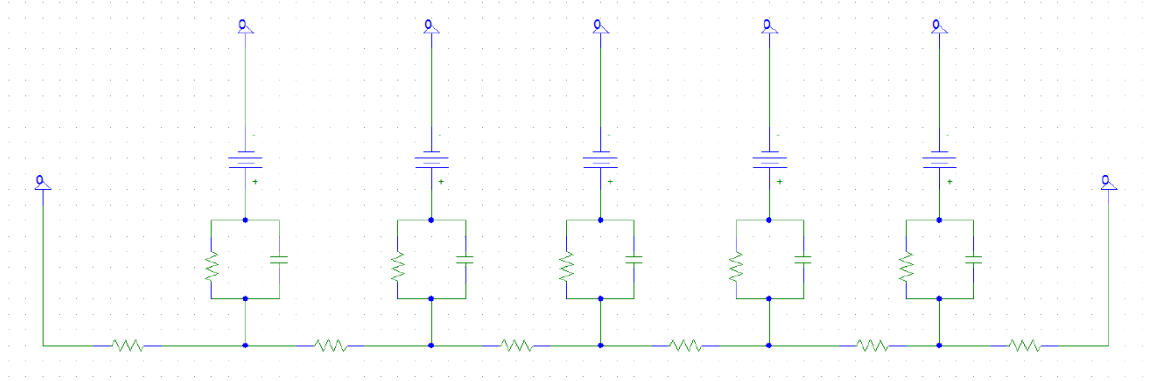


Figure 14: PSPICE schematics representation of an equivalent circuit model of a human myelinated axon. [35]

To better represent the human nerve fiber in a SPICE simulation, Nathan Angel presented a dissertation which aimed to model a myelinated/demyelinated HH neuron using the SPICE platform [1]. Angel worked to develop and implement a model of the human nerve in SPICE alone and did not include any work using an FEA tool. Specifically Angel worked using SPICE netlist code to develop a library that, when called, would function like a human nerve and output a valid action potential should the instigated stimulus be enough to reach threshold as seen in Figure 15 [1]. Nathan Angel accomplished the work of representing the human nerve in SPICE very accurately and for this reason his SPICE netlist code was originally chosen to be used in this work. Unfortunately, the limitations inherent to the COMSOL software, as previously described, forced the abandonment of the full HH model.

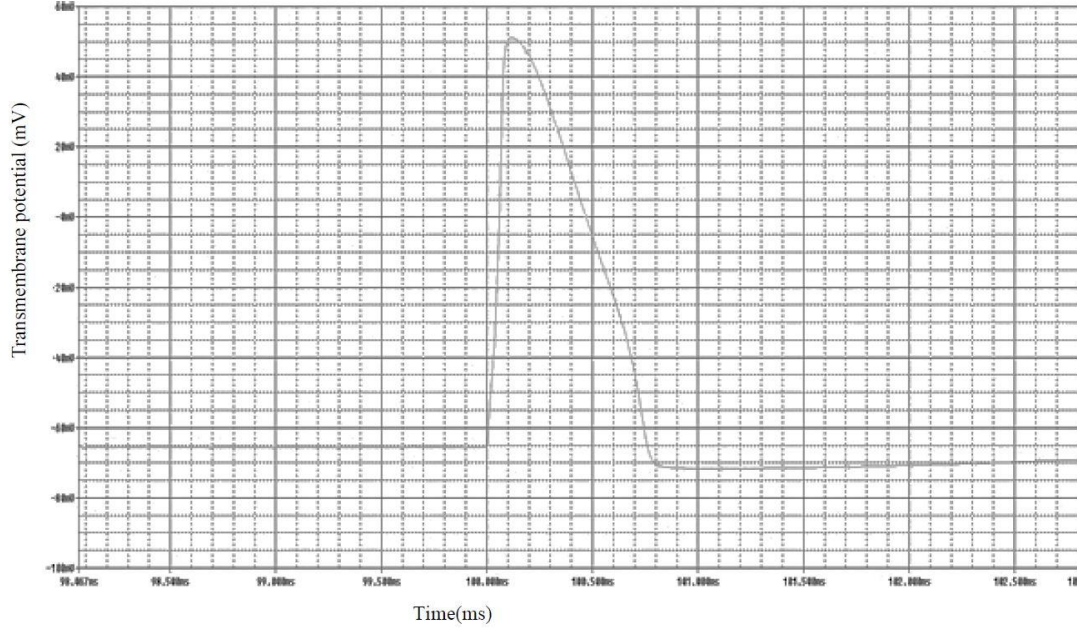


Figure 15: SPICE HH model of a neuron producing a characteristic action potential as developed and implemented by Nathan Angel. [1]

Using the HH model in SPICE netlist code was decidedly the most accurate representation of the system under study but there exists an example of a different approach in coupling COMSOL software with the HH model. In 2008 the journal of Artificial Organs published a short article that discussed the option of using the general spatial HH model governing equation [25]. Martinek et al. used the governing equation

$$C_m \frac{\partial V}{\partial t} = \frac{r}{2\rho} \frac{\partial^2 V}{\partial x^2} + g_{Na} m^3 h (V_{Na} - V) + g_K n^4 (V_K - V) + g_L (V_L - V) \quad (21)$$

to spatially represent the HH model along the longitudinal distance x [25]. The authors decided to develop a 1D representation of a muscle fiber and apply the provided spatial equation (21) to that fiber [25]. After the 1D fiber was created, it was singularly evaluated and then inserted into a rectangular 2D bulk volume conductor and later into a 3D volume conductor, similar to the work of Nathan Soto [25]. Within the 2D and 3D

volume conductors, Martinek et al. discussed the topic of coupling as is useful and valuable in the COMSOL software but did not extensively describe how this process was successfully accomplished [25]. Solving the simulation did evidently yield a characteristic action potential curve along the muscle fiber as seen in the intracellular potential in Figure 16, but the explanation of how the simulation was created and how the physics were coupled was lacking [25]. This lack of supporting information from Martinek et al.'s work shifted the emphasis to the SPICE netlist code as the most accurate representation of the human nerve.

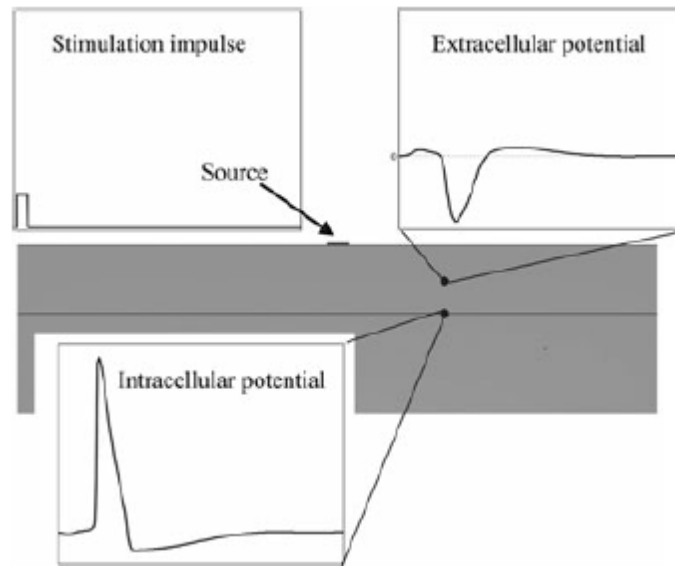


Figure 16: Resultant intracellular and extracellular potential from the applied stimulus pulse as done in the coupled 1D muscle fiber in the 2D bulk volume conductor. [25]

1.7 Project Objective

The model presented in this work uses SPICE netlist code to model an electric network that is coupled with an electric current volume conductor in COMSOL. To reiterate, it was originally hoped that the robust HH electrical model of a human neuron would be applicable in the continuation of this work but, to implement such an electrical circuit model, the segmented volume conductor must exist first. As a result, COMSOL

was used to create a segmented volume conductor model in the electric current module of the multiphysics program. It was discussed that such a model had not been previously used and that the human system had been treated as simply a bulk conductor. This work aimed to take the next step and divide the simulated arm into representative segments of the human anatomy including skin, muscle, nerve, and bone.

2 Methods

Understanding that this work is modeling a natural phenomenon and not accurate to the human system, it was believed that segmenting the model would yield more accurate results. With the segmented model developed and created, the next step was to incorporate and create the HH SPICE netlist code representing the electrical behavior of the nerve fiber membrane. Unforeseen restrictions, detailed below, inherent to the COMSOL software prohibited the use of the nonlinear HH model. In order to correct this deficiency, a linear SPICE netlist model needed to be developed to specifically incorporate COMSOL. Again, after several trials, a correctly functioning code was produced and the process of model coupling commenced resulting in a 2D electrical model of a portion of the human forearm successfully developed in COMSOL Version 3.5.

However, a system wide software update virtually eliminated the 3.5 version of the software. Since the coupling of the two systems was mostly dependent on the writing of SPICE netlist code in version 3.5, which included the subcircuit reference responsible for the integration, the 4.3 version of the software handled SPICE integration differently than its predecessor and did not allow the netlist code to function properly as written for version 3.5. As a result, the version incompatibility required that the model be discarded and a new model developed in version 4.3 from scratch. With the proper syntax applied in the netlist code and a newly created COMSOL model, the model coupling again was implemented and a working simulation of membrane electrical characteristics was created in COMSOL version 4.3 as presented in Figure 17.

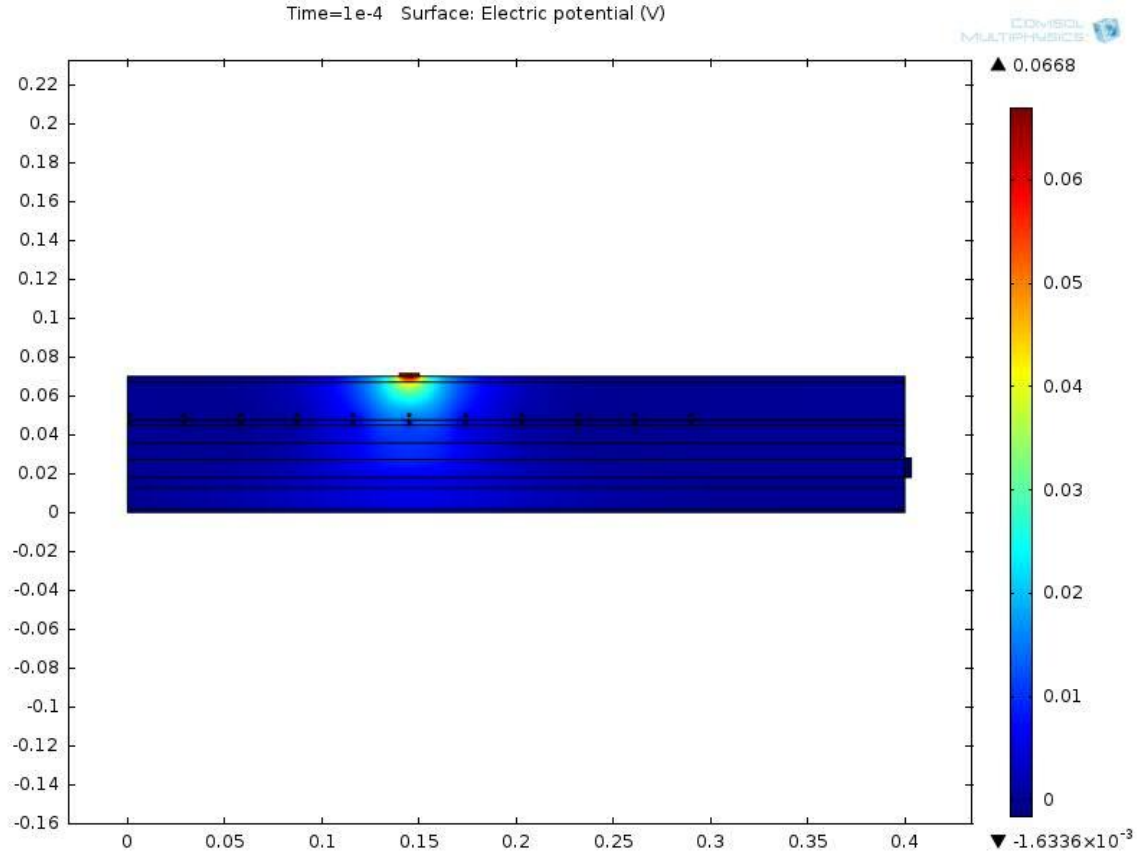


Figure 17: Resultant COMSOL simulation product of SPICE netlist code incorporated into a segmented volume conductor in version 4.3.

2.1 Two Dimensional COMSOL Model

The first step in working with COMSOL version 3.5 was to develop a 2D electrical model of a portion of the human forearm using a segmented volume conductor representation instead of a bulk model. To produce a segmented volume conductor, the initial task was to develop a 2D geometry for use in the simulation. The requirements were that it include the placement of a nerve, contain a geometry representing a stimulating medical electrode, and that it be representative of various tissue types. The median nerve trunk was selected for the model. A stimulating electrode was placed on top of the simulation domain to account for the current stimulus and also a grounding electrode was placed on the end of the geometry to be used as a reference ground during

both the finite element analysis and for use in the SPICE netlist. Segmenting the model was accomplished using a cross-section view of the human forearm for sizing and tissue placement. The cross-section view, separated along the axis in Figure 18, shows the median nerve along with five muscles, one bone, and two layers of skin. Excluding the connective tissue between the tissue layers, there remained the flexor sublimis digitorum, flexor profundus digitorum, flexor longus pollicis, extensor ossis metacarpi pollicis, extensor carpi radialis brevis, and radius bone. Using the average forearm diameter, 7.0824 cm, reported by Schell and Waterhouse as a starting point of the entire geometry, the dimensions of the biologic portions were found using a ratio system from the cross-section view [32]. This geometric calculation resulted in the height of each segment. The length of the model was taken from the work of Glenn Elert who established a mean length of 26.164cm for the human forearm [12]. A manual of nerve conduction studies was used for the electrode geometry placement and inclusion of a skin layer over the section of bone [5]. With the electrodes in place, the length was extended backward, disregarding the elbow, to a length of 40 cm which Soto indicated as being sufficient for maintaining convergence [35]. Finally with the geometry complete, the boundary and subdomain settings could be put in place.

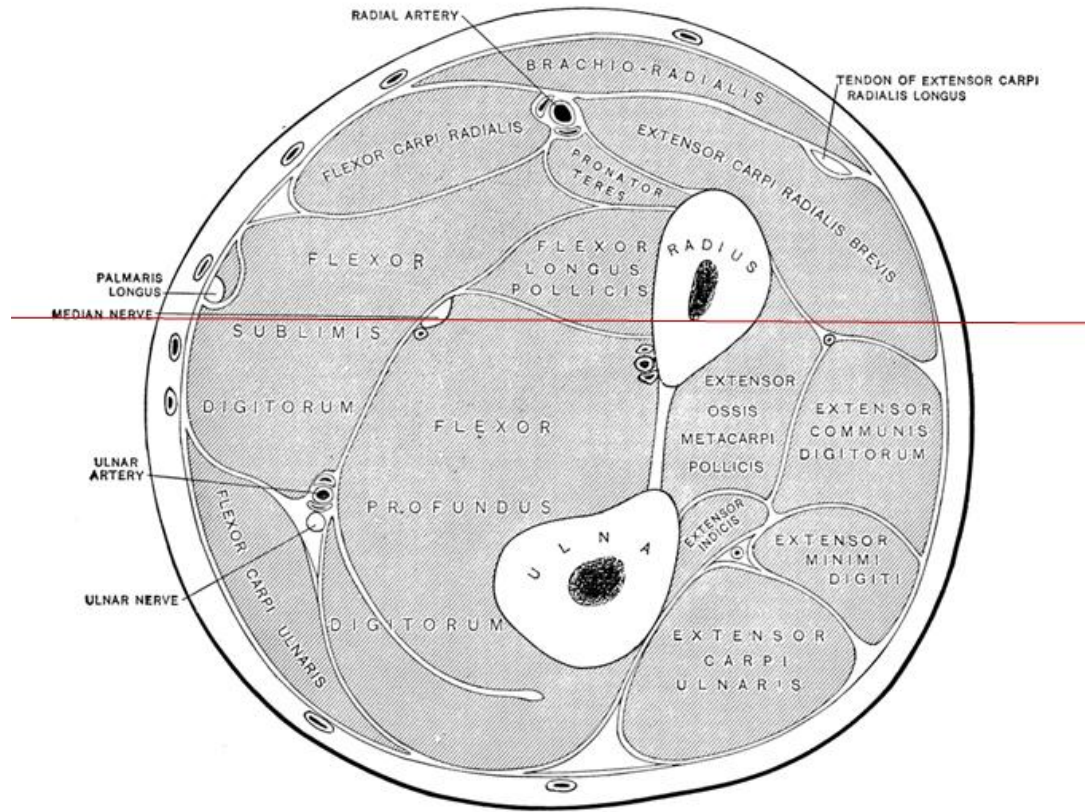


Figure 18: Cut view representation of the human forearm used as a model for geometry development. [24]

Boundary conditions in COMSOL are settings or conditions placed along the edges of each subdomain in the geometry. Usually the boundaries inside the model are continuous and therefore allow for solving throughout the geometry, leaving the outer surfaces as options. For this work, the top and bottom segments of the geometry were decidedly representative of human skin and as such their external boundary conditions were electrically insulating. Both outer surfaces of the medical electrodes were also electrically insulating. The next step was to declare all outer sides of the geometry as electrical grounds, provided that convergence was still observed using the length of 40cm as Soto's work suggests [35]. The ground electrode on the right side was also grounded at the skin contact point and the insulation boundary condition was applied to the outer

surface of the ground electrode. Finally the simulation required a form of excitation or stimulus and, to meet that requirement, the stimulus electrode on top of the geometry was labeled as a boundary current source providing a prescribed current density of $10^A/m^2$ to reach a current stimulus of 0.001A. Included in the final simulation were 22 separate circuit terminal boundary conditions applied to the added circular geometries in the 2D simulation that provided the connection to the SPICE netlist but were not present in the initial model. In the final model, eleven circular terminal boundary geometries were placed in the nerve subdomain and muscle subdomain, each as close to the represented membrane as meshing would allow. These added geometries communicated the circuit terminal boundary conditions to and from the SPICE netlist code but did not affect the subdomain electrical signal propagation as they shared the same subdomain settings as their respective surrounding tissue.

Each tissue carried a prescribed electrical conductivity and relative permittivity in its individual subdomain to account for the dielectric properties of the tissue. Like tissues were grouped together and assigned equal values. Therefore every muscle, both skin segments, and both electrodes, each respectively were assigned identical values for electrical conductivity and relative permittivity. It was discovered that the dielectric properties of tissues range greatly in value depending on the applied frequency. After consideration, it was decided that a frequency of 433 MHz would be used as Furse discusses that this is a commonly used frequency for Industrial Scientific Medical (ISM) applications [15]. Further still, the assumptions were made that dry skin was being modeled and that the bone was entirely cortical.

From these assumptions, the subdomain settings for the dielectric properties of the tissues were assigned specifically as follows in Table 2 [15]. As stated above, the circular geometries included in the final simulation had the same subdomain properties as their respective tissues. Finally, the subdomain settings of the two electrodes were allowed to remain as defaults since they represented an idealized conductor. As seen in Figure 19, each subdomain was assigned values for dielectric properties. Along with those properties, the segments were expanded in thickness to account for greater variability in solving, and therefore all segments, but the electrodes were given a thickness of 0.07 m while the electrodes were given a thickness of 0.01 m. While the thickness remained constant from COMSOL version 3.5 to version 4.3, an error occurred in the translation process relating to the values placed on relative permittivity. In version 3.5, the values were adjusted from 1 to their respective values expressed in Table 2. During translation to version 4.3, those specific values were lost and the simulation ran using the standard values of 1 for every relative permittivity.

Table 2: Dielectric properties of selected tissues at 433 MHz. [15]

Tissue	Relative Permittivity	Electrical Conductivity (S/m)
Bone (cortical)	13.77	0.1032
Muscle	64.21	0.9695
Nerve	35.70	0.500
Skin (dry)	42.48	0.5495

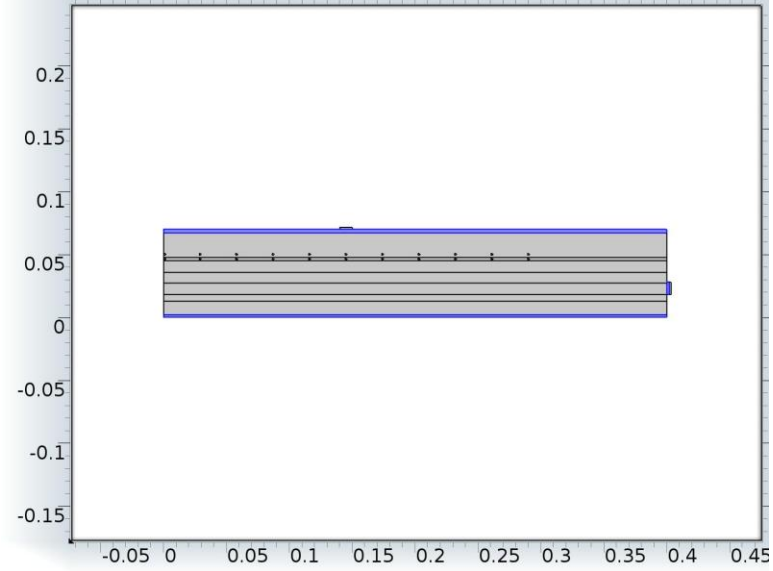


Figure 19: Subdomain selection of the skin segments on top and bottom of the model and the small segment between the bone and ground electrode on the side to better simulate a natural occurring ground electrode.

The error was not discovered due to the output being nearly the same between versions. Also, the simulation produced a result that was not only qualitatively but also quantitatively closer to the desired outcome of a more accurate representation of the natural phenomena. The results suggest the changes in relative permittivity had a minimal impact on the simulations. Finally, the purpose of this work was to present an advanced computational model of human neural recruitment and excitation through the coupling of electric current signal propagation in the COMSOL Multiphysics software with human neural membrane electrical characteristics represented in SPICE netlist code. It is the action of representing human neural membrane electrical characteristics that formed the bulk of this work's progress towards its purpose.

2.2 SPICE Netlist Neural Modeling

SPICE netlist code was developed using PSPICE software to best model the electrical characteristics of the human neural membrane as mentioned, first using the advanced HH model, and later, using the linear representation presented by McNeal and

expanded upon by Szlavik [26, 37]. The attempt at adapting the full HH model to COMSOL's constraints was performed based on the work of Angel [1]. As stated before, Angel developed a library or subcircuit file to be used in conjunction with a source circuit netlist code [1]. Creating a subcircuit interface allowed the human neural membrane model to be used in this project. In applying the electrical network as described and developed in Angel's work to the developed 2D COMSOL model, it was reasoned that the current source statement, as seen in Figure 20, would be the only item that required adjustment. This assumption is where the deficiencies inherent to the functionality of COMSOL resulted in a total re-working of the simulation.

```
.OPTIONS NUMDGT=6

* Cell Length (m)
.PARAM LENGTH={ (80.0E-6)*100}

* Cell Radius (m)
.PARAM RADIUS={ (10.0E-6)*100}

* Injected Current Magnitude Per Unit Area (A/cm^2)
.PARAM AMPL=0.0

* Math Constant
.PARAM PIE=3.14159

* Calculated Stimulus Current Amplitude (A)
.PARAM STIMAMP={ (2*PIE*RADIUS*LENGTH + 2*PIE*RADIUS^2)*AMPL}

I1 0 1 pulse(0 {STIMAMP} 0 0 0 0)
RD 1 0 1.0E10

xsub      1 0 NEURON

.LIB Neuron_5.LIB

.tran 20.0E-6 20E-3 0 1E-6
.probe V(1)
.END
```

Figure 20: Electrical current source statement written in SPICE code to be used with the included "Neuron_5" library.

In attempting to import and implement the created electrical circuit neural model, it was discovered that COMSOL inherently placed a number of restrictions on SPICE netlist circuitry code. COMSOL prohibited the use of:

- Scientific Notation
- Negative Signs

- Non-basic Syntax
- Variable Declarations
- Library Attachments
- Initial Conditions
- Equation Solving Capabilities

As such, the represented membrane electrical characteristics, as shown in Table 3, were unable to be correctly modeled. The included ".PARAM" statements, along with all initial conditions, "value" calculations, negative signs, and scientific notation had to be re-evaluated. Scientific notation statements were easily replaced using decimal values. Negative signs were originally only used in voltage statements and were removed to create positive voltages that would be accounted for prior to simulation. The restriction of library attachments was easily circumvented in that the electrical current source code was combined with the neural characteristic code. Variable declarations of ".PARAM" statements were excluded and variable references were replaced with decimal values. However, all "value" calculations, initial condition statements, and equation solving parameter statements were excluded and could not be replaced because a possible solution in the SPICE importing routine did not exist. Without the functionality of the "value" calculations, the capabilities of the HH model were negated and the netlist code became invalid and useless which necessitated the use of a simpler linear model as seen in Figure 21. As the simulation progressed, calculations using "value" statements accounted for changing voltage relationships which can be seen in the EAN quantity description in Table 3. Equation solving capabilities were only possible through the

coupling of COMSOL derived equations. Initial conditions were assumed to be possibly dismissible but the "value" calculations exclusions were prohibitive.

a)

```
.SUBCKT NEURON 31 30
.PARAM CAPPUA=10.0E-7

*****
*
* coNa = 491.0E-3      Extracellular sodium concentration (mol/L)
* ciNa = 50.0E-3       Intracellular sodium concentration (mol/L)
* coK  = 20.11E-3      Extracellular potassium concentration (mol/L)
* ciK  = 400.0E-3      Intracellular potassium concentration (mol/L)
*
* GNaMax=120.0E-3
* GKMax =36.0E-3
*
* U_r = -62.5E-3       Resting Membrane Potential (V)
*
* Temp = 6.3           Temperature (Degrees Celsius)
*
* b = 0.02             Relative permeability of sodium to potassium
* R = 8.314            Reiberg gas constant (joules/(mole*kelvin))
* Z = 1.0              Sodium and potassium ionic valence
* F = 9.6485E4         Faraday's constant (coulombs/mole)
*
*****

.PARAM HO=0.0393
.PARAM HO=0.6798
.PARAM HO=0.2803

.PARAM UMO=-55.0E-3
.PARAM UK=-72.0E-3

*****
* CALCULATED PARAMETERS
*
.PARAM CELCAP=((2*PIE*RADIUS*LENGTH + 2*PIE*RADIUS^2)*CAPPUA)

*****
FNA 31 27 UINA 1
FK 31 28 UIK 1
UNK 28 30 {UK}
UNNa 27 30 {UNa}

ENAK 26 0 31 30 1
CE 31 30 {CELCAP} IC=-62.5E-3

*Sodium current current pathway
*H variable
CM 2 0 0.26E-3 IC={HO}
RN 2 0 1E10

GAN 0 2 POLY(2) 2 0 5 0 0 1 0 -1
GBH 0 2 POLY(2) 2 0 6 0 0 0 0 -1

EAM 5 0 value=(-0.1*(v(26)*1E3+35)/(exp(-0.1*(v(26)*1E3+35))-1))
RAN 5 0 1E10
```

b)

```
McNeal Current Sources 20micron Diameter Fiber

* Fiber Diameter (m)
* Pulled from Figure in Szlavik Paper "The effect of stimulus current pulse width on nerve
* fiber size recruitment patterns"
.PARAM FIBERDIA=0.0002

* Cytoplasm Resistivity (ohm-m)
.PARAM CYTORES=1.1
* Membrane Conductance (S/m^2)
.PARAM MEMCOND=300
* Membrane Capacitance (F/m^2)
.PARAM MEMCAP=0.02
* Node of Ranvier Width (um)
.PARAM NODEWIDTH=0.000025
* Ratio of axon to fiber radius
.PARAM AFRATIO=0.7
* Current Source Parameter (A)
.PARAM CURRENTSOURCE=0.015
* Axon Diameter (m)
.PARAM AXONDIA=(AFRATIO*FIBERDIA)
* Fiber Radius (m)
.PARAM FIBERRADIUS=((0.5*FIBERDIA))
* Axon Radius (m)
.PARAM AXONRADIUS=((0.5*AXONDIA))

* Node of Ranvier Spacing (m)
.PARAM NODESPACE=(100*FIBERDIA)
* Equivalent Axoplasm Resistance (ohm)
.PARAM EAXORES=((CYTORES*NODESPACE)/(3.14159265359*(AXONRADIUS^2)))
* Equivalent Membrane Resistance (ohm)
.PARAM MEMRES=((1/(2*3.14159265359*MEMCOND*AXONRADIUS*NODEWIDTH)))
* Equivalent Membrane Capacitance (F)
.PARAM MEMCAP=((2*3.14159265359*MEMCAP*AXONRADIUS*NODEWIDTH)))

*****
R01 1 201 290850.3317 ;Membrane Resistance
C1 1 201 0.00000000226194671 ;Membrane Capacitance

*Axoplasm Resistance 1
R01 1 2 1867417999

*120 0 300 pulse(0 0.0001 0.00001 0.00001 0.00001 0.00008 0.0005)
*TRAM 0.0000001 0.0025

*****
R01 0 101 {EAXORES}

U1 1 0 pulse(0 0.05 0 0.00000001 0.00000001 0.0005 0.001)
*U = - pulse(initialvoltage pulsedvoltage delay Falltime risetime pulsewidth period)
R1 1 101 {MEMRES}
C1 1 101 {MEMCAP}
*U11 111 111 0.07

R02 101 102 {EAXORES}

U2 2 0 pulse(0 0.05 0 0.00000001 0.00000001 0.0005 0.001)
*U = - pulse(initialvoltage pulsedvoltage delay Falltime risetime pulsewidth period)
```

Figure 21: a) Partial representation of robust HH model of human electrical neural characteristics as developed by Nathan Angel under the direction of Dr. Robert Szlavik. b) Linear netlist circuitry code partial representation of created model of human neural membrane electrical characteristics.

Table 3: Biologic membrane electrical characteristics of potassium ion channel values used in the SPICE neuron model presented as an example of the advanced functionality not allowed by COMSOL.

Potassium channel variable	Description	Quantity
V_m	Measured potential across membrane	$V_{\text{outside}} - V_{\text{inside}}$
ENAK: voltage controlled voltage source	Potential across membrane	$V_m = V_{\text{outside}} - V_{\text{inside}}$
EAN: voltage controlled voltage source	α_n voltage relationship	$\alpha_n = \frac{-0.01(V_m + 50)}{e^{-0.1(V_m + 50)} - 1}$
EBN: voltage controlled voltage source	β_n voltage relationship	$\beta_n = 0.125e^{-0.0125(V_m + 60)}$
GAN: voltage controlled current source	α_n rate equation term	$\alpha_n(1 - n)$
GBN: voltage controlled current source	β_n rate equation term	$-\beta_n n$
CN: capacitor	Time derivative for n gate, and temperature constant ϕ	$C_n = -(1/\phi) \frac{dn}{dt}$
EN4: voltage controlled current source	n gating variable to the fourth power	n^4
E_K : Constant voltage source	Battery potential for potassium	$E_K = \frac{RT}{F} \ln\left(\frac{c_K^o}{c_K^i}\right)$
EMK	Difference of battery and membrane potential	$V_m - E_K$
I_K : Voltage controlled Current Source	Current through potassium channel	$G_K = \bar{G}_K n^4 (V_m - E_K)$
VIK: Voltage controlled Voltage source	Potassium ionic current	I_K

Linearization of the netlist circuit both simplified the analysis and allowed for importing into the COMSOL software. Included in the linear code are the variable declarations and calculations for the values as seen in Table 1, which established correct membrane resistance and capacitance, and axoplasm resistance values during the development process. Once prepared for import into COMSOL, such variables were replaced in the circuit component declarations with their respective values. Such

respective values were calculated as seen in Table 1 from the work of Szlavik, based off the work of McNeal [37, 26]. Originally, McNeal presented an electrical network representation of a myelinated nerve fiber containing the RC characteristic membrane network in parallel, separated by axoplasmic resistances, all excited by injected voltage sources as seen in Figure 7 [26]. Szlavik presented a very similar network model of a section of myelinated axon without the injected resting membrane potential sources of -70 mV, but did include a graphic to assist in the location of the nodes of Ranvier in Figure 8 [37]. It is this simplified circuit model, that was expanded from three nodes to eleven and grounded on either end, that was imported into COMSOL. Replacing the voltage sources in the coding were eleven separate subcircuit node connections to the COSMOL simulation pulling in direct current (DC) values as seen in Figure 22.

Originally working in version 3.5 of COMSOL, the injected current source was the result of the circuit network combined with the voltage source nodal connections. However, combining the voltage source nodal connections with the circuit network was not easily possible in version 4.3 so a piecewise continuous function was implemented and called as a boundary current source property in the simulation. Modeled after the original SPICE current source, the function was thus: $\{ \{0, 0.00000001, 0.1 \cdot x\}, \{0.00000001, 0.0005, 8.5\}, \{0.0005, 0.00050001, -0.1 \cdot x\}, \{0.00050001, 0.001, 0\} \}$ producing the pulse function as seen in Figure 23. The ground electrode connection was still implemented in the netlist circuitry as a reference for both the SPICE and COMSOL simulation.

Connecting the ground node followed the same syntax and process as the voltage source nodal connections. Finally, to communicate the resultant membrane potentials back to COMSOL to complete an iterative cycle, a series of eleven voltage controlled voltage

sources with gains of one were created dependant on the nodes above and below the RC network representing the neural membrane. To finish and correctly simulate the nerve fiber activation, the resultant resistors were connected from ground to the output node of each of the voltage controlled voltage sources. These final adjustments would account for half of the coupling performed in the simulation.

```
*Connection to COMSOL
*
.SUBCKT NoRs      NoR1      NoR2      NoR3      NoR4      NoR5      NoR6      NoR7      NoR8      NoR9      NoR10     NoR11     COMSOL: *
.ENDS
*Connecting COMSOL nodes into circuit for Nodes of Ranvier
X1 1 2 3 4 5 6 7 8 9 10 11 NoRs
```

Figure 22: SPICE circuit netlist coding responsible for COMSOL nodal connections of voltage sources.

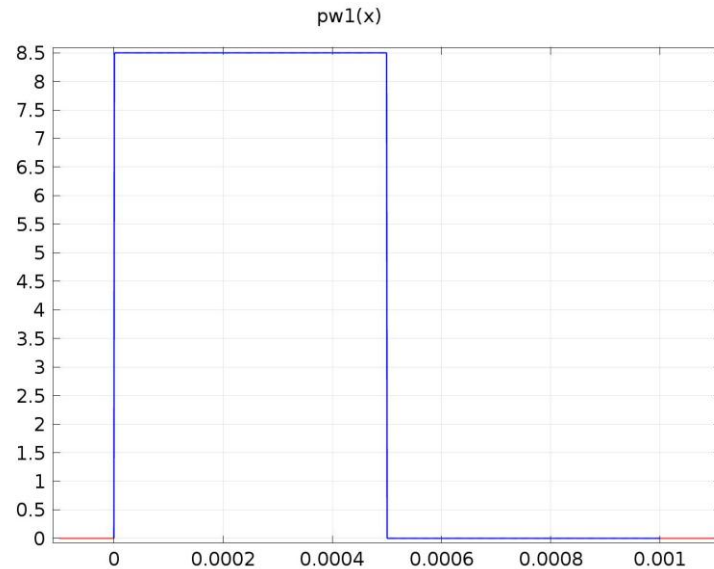


Figure 23: Piecewise continuous function created to serve as the pulse current source necessary for correct neural simulation.

2.3 COMSOL to SPICE Coupling

The other half of the coupling performed was done through syntax created specifically for that purpose in COMSOL version 4.3 since COMSOL 3.5 required only the subcircuit references to create a coupled model. In version 4.3, there existed a relatively simple method of calling variables from another physics module. Specifically

in this instance, it called the imported SPICE netlist code. In total, half of the coupling was done using circuit terminal boundary conditions set to input voltage sources into the SPICE electric circuits module, and the other half was accomplished using this described syntax of calling the continuous values of a variable inside the electric circuit physics module. To call those continuous voltage values, eleven terminal boundary conditions were placed just below the modeled membrane and inside the modeled nerve segment that was used to communicate voltage values from the electric circuit physics module to the electric current physics module. Set apart, and just above the modeled membrane, were another eleven terminal boundary conditions that were used as voltage sources from electric currents to electric circuit physics module. As is now evident, this process of passing voltage values to and from different physics modules implemented the coupling action and was partly accomplished by the described COMSOL syntax.

Calling voltage values from the electric circuit physics module using COMSOL syntax required only an input of the corresponding potential difference across the resistors placed between ground and the output of the aforementioned voltage controlled voltage sources. Those resistors were labeled "RT(x)" where x is replaced by the corresponding NoR number, from one to eleven. Each resistor held a value of only a single ohm, which is not a realistic value but allowed for a small potential drop across each resistor. Transmitting resistors, as the title "RT" stands for, provided a voltage value input back into the electric currents physics module using the syntax of "mod1.cir.RT1_v." Standard in calling electric circuit elements from the current model is the "mod1" and "cir" syntax. "RT1" calls transmitting resistor one for node of ranvier one and finally the "_v" dictates a voltage value, not current, be passed. This membrane

potential is what created the RC characteristic response necessary in modeling linearized human neural membrane electrical characteristics. Therefore it is at these terminal boundary condition nodes of ranvier that the simulation is fully coupled and the purpose of this work achieved. Finally, to compute the result with a coupled simulation, the model geometry was meshed and solved to realize a final solution.

2.4 Geometry Meshing

Meshing the geometry was the first step in realizing the goal solution of the 2D COMSOL and SPICE coupled simulation. Meshing was performed using the built in functionality of the COMSOL software which allowed for a choice between nine different mesh options. The nine options were:

1. Extremely Fine
2. Extra Fine
3. Finer
4. Fine
5. Normal
6. Coarse
7. Coarser
8. Extra Coarse
9. Extremely Coarse

Each mesh selection provided a different level of resolution through a larger number of elements in the mesh. Mesh element number selection is necessary in determining solution convergence and is a common feature of FEA software. In other words, there exists a number of elements for which exceeding that number does not enhance the

accuracy of the simulation. That number of elements is found through a mesh convergence plot which evaluates the same problem multiple times using varying numbers of elements in the mesh. In general, as the number of elements grows, so does the accuracy and required computing power. Finding this useful mesh convergence data was done through the built in COMSOL mesh selection options in conjunction with Microsoft Excel. Comparing the number of elements to a point evaluation of voltage, as will be explained in detail in the following paragraph, provided the ideal number of elements as found through mesh convergence.

Simulations began using the coarsest mesh option available in COMSOL to save time and computing power during simulation trials. Choosing an extremely coarse mesh provided a number of elements equal to 9446. Using the selection of extremely fine mesh, the maximum number of elements created was 80192 which is where the voltage values began to level off to a final 0.00931 V. Figure 24 illustrates that the number of degrees of freedom needed to create an accurate solution should be around 70,000 which correlates to around 37,000 number of elements.

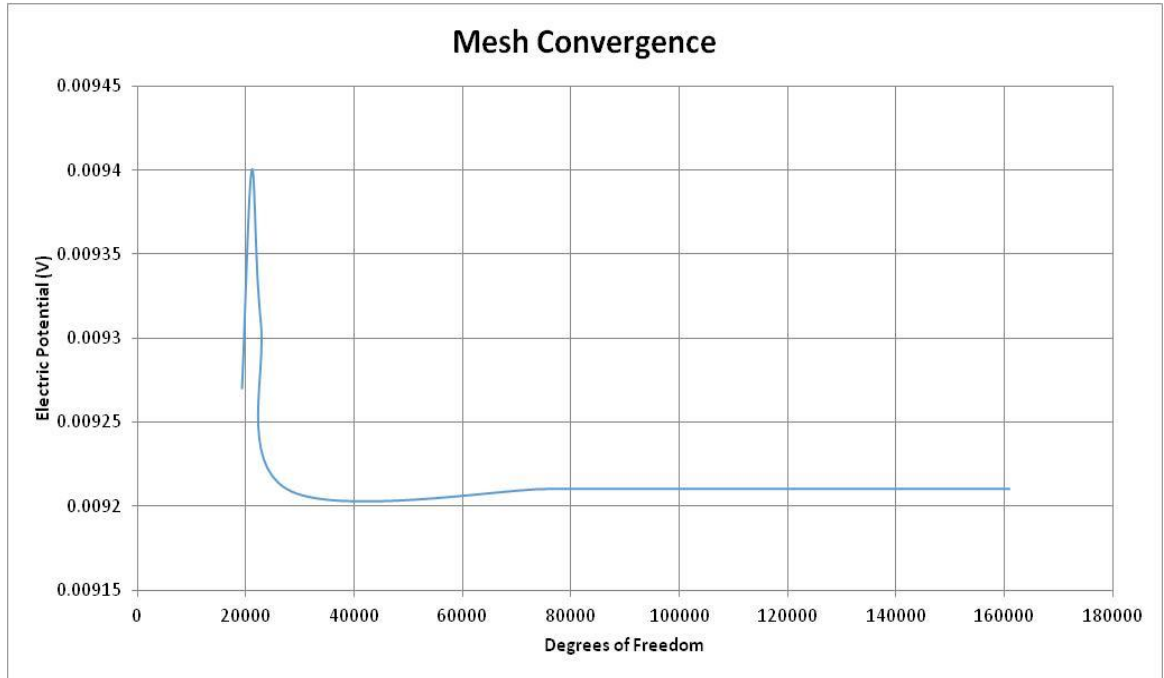


Figure 24: Mesh convergence plot created in Microsoft Excel using data generated in COMSOL Multiphysics.

The decision was made to move forward with a number of elements equal to 13541, or around 30,000 degrees of freedom, due to the resultant voltage value equaling the rest value at that number of elements. At 13541 elements, the point voltage value was found to be 0.00921 V and the time to solution was four minutes and thirteen seconds using the mesh choice of coarse. Establishing a maximum element size of 0.0403 m, the final mesh selection is seen in Figure 25. With a final mesh selected, the next step was to determine the correct solver that had to be used.

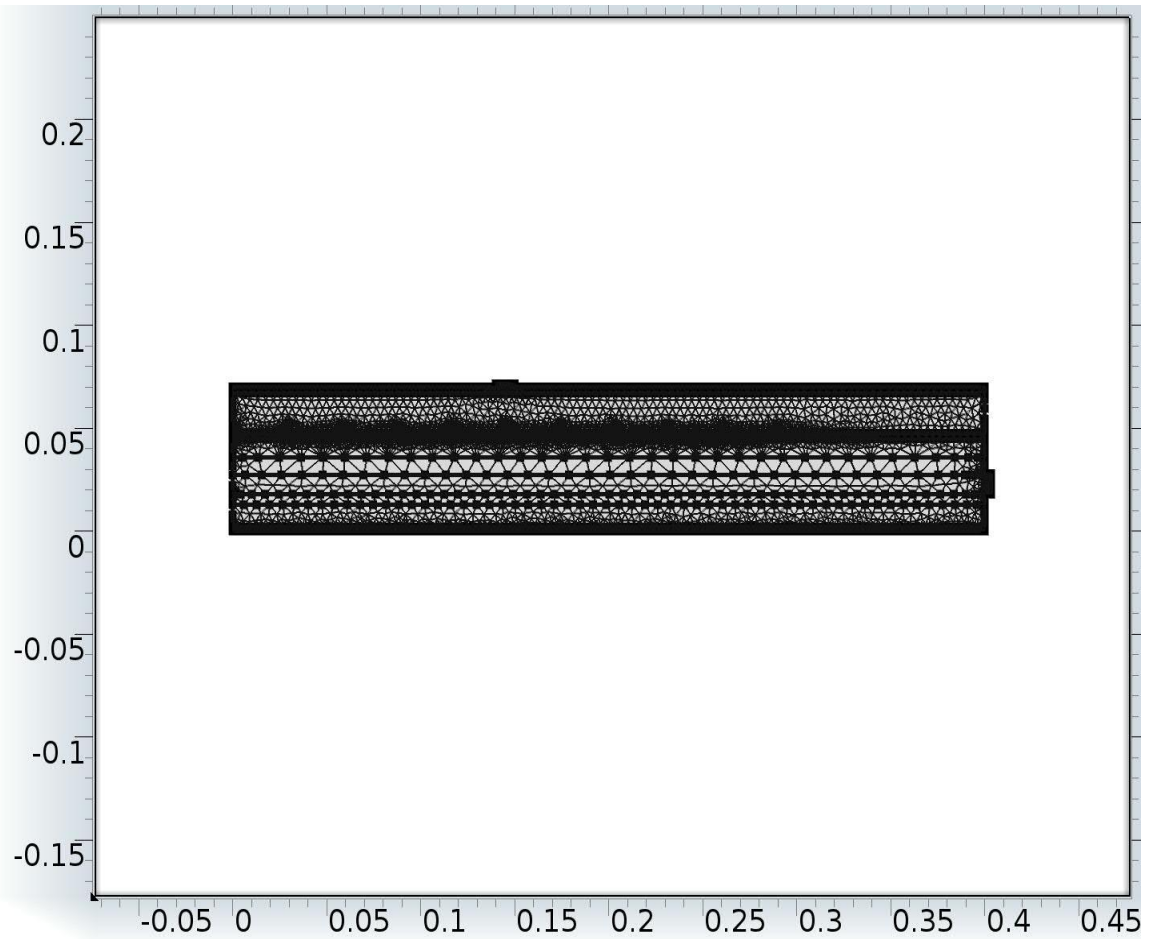


Figure 25: Mesh geometry of developed COMSOL simulation describing a cut view of a human forearm.

2.5 Simulation Solving

COMSOL provides a number of choices for solvers for solving finite element simulations including, but not limited to: stationary, eigenfrequency, frequency domain, linear, nonlinear, and time dependent solvers. Due to the nature of this work, a linear time dependent solver was used to account for the time dependent voltage differences created by the pulse current source and the linearity of both the FEA and SPICE portions. A near identical current pulse was implemented in the SPICE netlist circuitry trial as was used in the COMSOL simulation which produced nearly identical results in terms of time dependency. Also, SPICE netlist code used the syntax ".TRAN" to specify a transient

analysis of the proposed circuit network in called time steps of 1 microsecond up to 1000 microseconds. Implemented in COMSOL, the solver contained the syntax "range(0,1.0e-6,0.0010)" detailing an evaluation starting time of 0 seconds, time step of 1.0e-6 seconds, up to a final 0.0010 seconds, thus matching the specification in SPICE. Matching the solvers ensured that the results would be comparable.

Also required to assure comparable and viable results, was an adjustment of the relative tolerance of the solver from a default 1 to 0.00001 volts. A smaller tolerance forced greater numbers of iterations to find solutions within a range of 10^1 V. Because the range of values for the results was in the millivolts, a tolerance of a volt was too far out of range to provide accurate solutions therefore the relative tolerance was decreased. Using a finer tolerance provided a more accurate solution with 27498 degrees of freedom solved for. Finally, with the time stepping correct and the tolerance adjusted, the only setting that remained to be specified was to ensure that a fully coupled solver was used. Fully coupling the solver was necessary to produce accurate results because the simulation was designed specifically to implement an iterative coupling between the SPICE netlist code and the COMSOL domain settings. Solving the simulation in this fashion produced viable results in the form of potential simulations throughout the model.

3 Results

The results of the computational model of human neural recruitment and excitation implemented in COMSOL Multiphysics and SPICE software, are presented below. Included is a summary of the results of the work performed over many trials and not a detailed description of the results from each iteration. The figures associated with the final results are presented at the end along with a description of the attainment of the desired solution as compared to the published literature previously outlined.

3.1 Final Result Presentation

Presented here are the potential measurement profiles developed through the coupled COMSOL-SPICE simulation. Using the voltage values measured from the induced boundary current source in Figure 17, a potential profile was created showing the measured voltage values at the boundary current source. Comparing the piecewise continuous function displayed in Figure 23 and the induced boundary current source displayed in Figure 26, it is clear that the boundary current source closely matches a pulse source characteristic square wave.

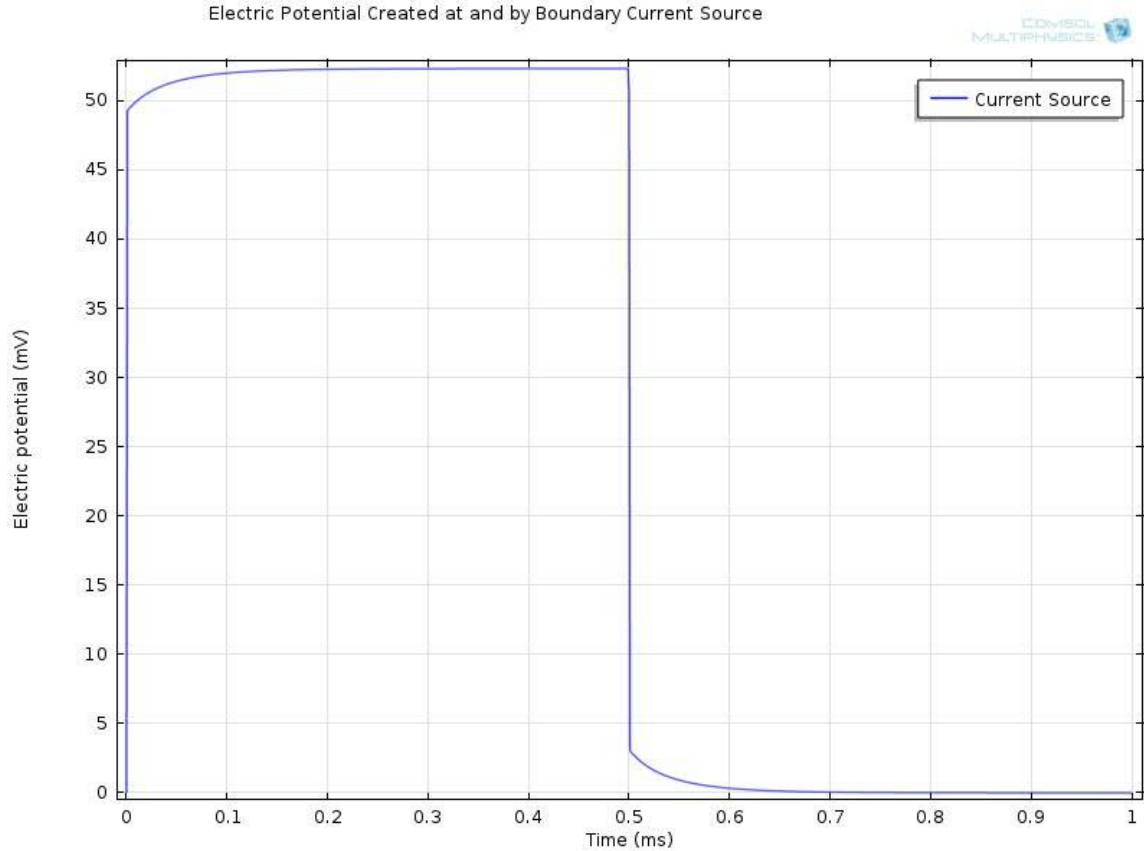


Figure 26: Boundary current source potential profile created from COMSOL.

Beyond the boundary current source, another eleven modeled sources existed in the simulation. Those eleven sources, as seen as upper points in Figure 17, were created by using the voltage values from the electric currents module in the electric circuit module as voltage to ground measurements displayed in Figure 27. The difference between these and the boundary current source is the simulated voltage variable rather than current. Voltage and current measurements are still related mathematically using Ohm's Law as described in Equation (1) inside a resistive medium. A resistive medium, such as the geometry implemented in COMSOL, facilitated the coupling of the electric currents module and electric circuit module to produce an iterative solution, or membrane potential profile, when used with the voltage simulations seen in Figure 27.

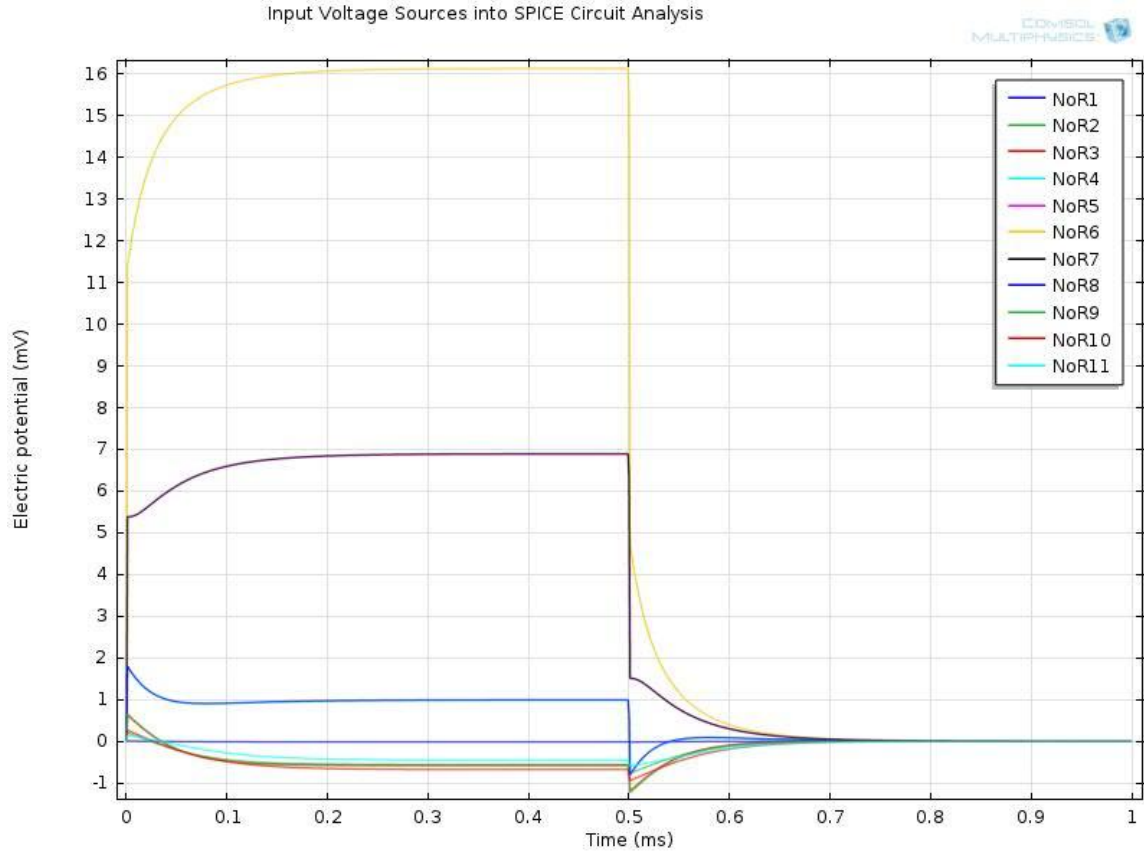


Figure 27: COMSOL created voltage to ground measurements in the electric currents module translated to grounded voltage sources in the electric circuit module.

For reference, when using the aforementioned linear model of the human nervous membrane, a potential profile should display the RC characteristic curvature as seen in McNeal's work [67]. McNeal presented a calculated solution to the linear model [26]. Presented in Figure 28, this calculated solution shows the goal for quantitative and qualitative comparison. The solution is a potential profile of the McNeal model of the human nervous membrane. For comparison, a set of membrane potential profiles were generated in COMSOL at the boundary conditions, or separations between segments, located in the nervous geometry. Voltage measurements of the induced voltage sources were taken at the boundary conditions just above the modeled membrane rather than just below. For ease of use, the membrane potential measurements taken just below the

membrane, inside the nervous geometry, were labeled identically as illustrated in Figure 27. When comparing Figure 29 to Figure 28, also note that the time scale in Figure 29 is a magnitude of 10 off that of Figure 28 in that 1 ms does not equate to 100 μ s.

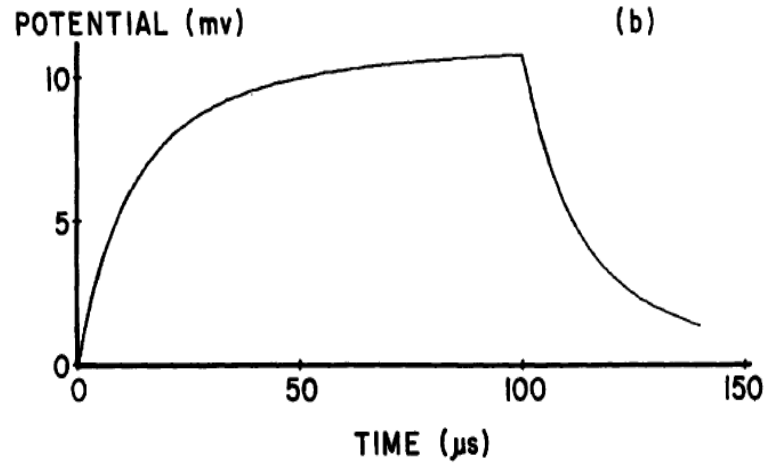


Figure 28: McNeal calculated solution for control comparison in simulation analysis. [26]

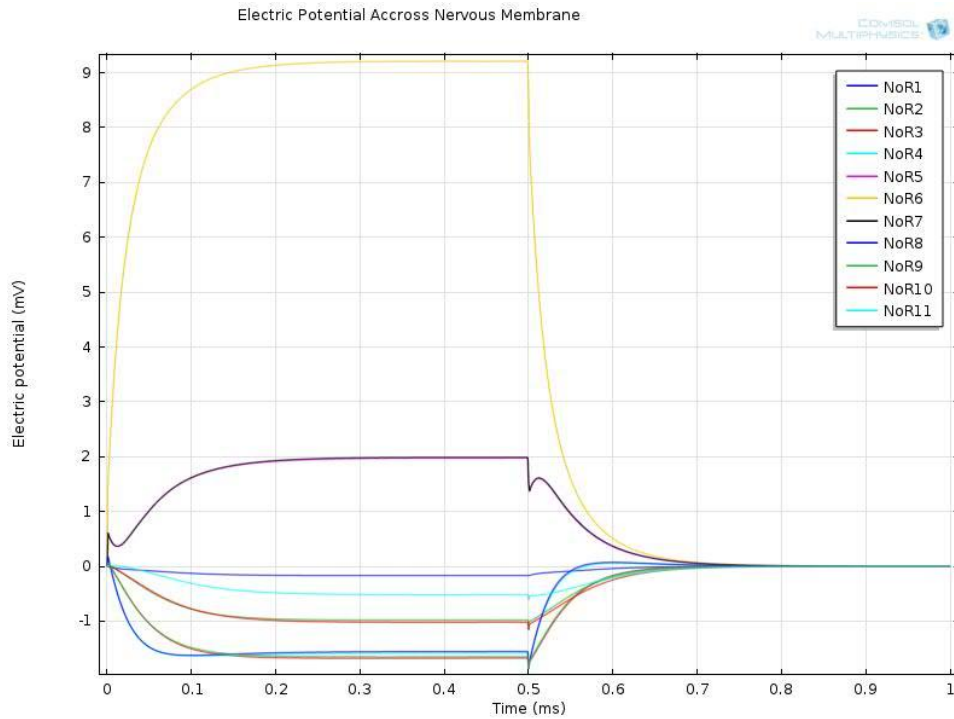


Figure 29: COMSOL generated human nerve membrane potential profiles.

Finally, to aid in the most direct comparison to McNeal's solution, in Figure 28 a graphical representation of the time varying potential at the membrane terminal directly below the source was generated. Seen in Figure 29 as the profile of NoR6, the result is presented in Figure 30 alone, without other profiles for direct comparison to McNeal's work.

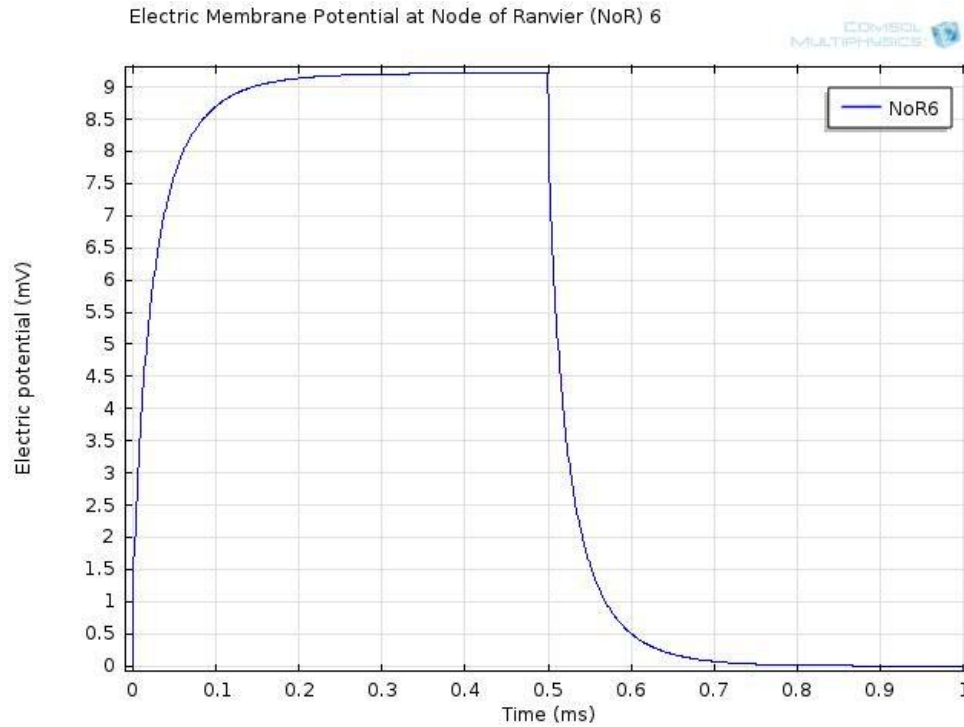


Figure 30: Electric potential profile of the terminal boundary condition located directly below the current source.

4 Discussion

The purpose of this work was to present an advanced computational model of human neural recruitment and excitation through the coupling of electric current signal propagation in the COMSOL Multiphysics software with human neural membrane electrical characteristics represented in SPICE netlist code. McNeal's work had the purpose of providing an adequate model for describing nerve excitation up to the initiation of an action potential and was used as a foundation for this work [26]. In an attempt to most accurately reach that goal, a 2D simulation in COMSOL was built and linear SPICE netlist code was incorporated. It is this coupled simulation that produced the final potential profiles describing nervous excitation due to injected current throughout a simulated biologic tissue. Current was injected via a devised boundary current source setting and sourced from a constructed piecewise continuous function. The voltages induced from the electric current flowing through the resistive media were used as DC sources in the SPICE network of the neuron. Those sources established a simulated membrane potential similar to McNeal's original work.

4.1 Boundary Current Source

The boundary current source as presented in Figure 26 was the first step in establishing this comparison between these results and that of the literature. The imposed boundary current source was based off of the piecewise continuous function detailing a square wave pulse. Therefore the current emitted from the boundary source should be pulse-like in nature, as illustrated in Figure 23, but resulted in a slight slope at the beginning of the pulse and at the end of the pulse as illustrated in Figure 26. This slight slope is consistent with what would be expected from the electrical characteristics of the

neuron. A square function did produce a square wave but the RC characteristic response coupled back to the system accounted for the exponential rise time associated with the pulse. RC response in the pulse source is noticeably smaller than the membrane potential curvature because the electric signal was forced to travel through a large amount of resistive media from the originated terminal boundary conditions to the source. This greatly decreased the strength of the electrical signal and thus the RC response of the induced wave.

Inducing the RC response as seen in Figure 26 was achieved using potential values of voltage and not current values of amperes so the boundary current source resultant wave was presented as a plot of voltage and not current. Presenting the boundary source as a plot of voltage and not current was also necessitated by the rest of the simulation being performed as an analysis of voltage values. Conductance, the inverse of resistance, was quantified and considered in this simulation and thus the simulation was one of a resistive media. This simulation of a current source in a resistive media could be translated to voltage using Ohm's Law.

4.2 Voltage Source Inclusions

Time varying voltage simulations were taken at the terminal boundary conditions and converted into voltage sources in the neural circuit. The results are displayed in Figure 27. Each source had a different potential value that was communicated to the circuit. Communication of potential values to the circuit was due again to the resistive nature of the simulation geometry. As the electrical signal traveled away from the source, the resistive properties of the various conductive media altered the signal. Normally when a source is passed through a resistance, a reduction of signal strength occurs. Due to

added variables in the simulation created by the coupling of the electric currents module and electric circuit module, irregular alterations to the signal occurred. Along the length of the geometry, simulated biologic tissue resisted the transmittance of the electric signal. Certain biologic components, like the nervous membrane described using SPICE netlist code, added a capacitive component to the signal resulting in the exponential rise times.

The RC response created by the coupling of the simulated biologic tissue and nervous membrane accounts for the shape of the imposed waves. In the same process as was seen with the boundary current source, the generated voltage sources from the network simulation carried a similar response into the network simulation. More specifically, the network produced the RC response, which was then transmitted through the COMSOL conductive media to the voltage sources and back into the SPICE circuit network which produced the unexpected RC response seen in the induced voltage sources. COMSOL's iterative solver is what created this unexpected transmission of an RC response through the conductive media. Such unexpected outcomes create opportunity for future academic work but do not disqualify the choice of solvers in this work.

An additional issue that resulted from the complexity of the iterative solver was that a number of the induced voltage sources produced a negative voltage in the simulation. The negative voltage inputs are to be expected after an initial spike in potential due to the current source initialization which is due to the distant nodes of ranvier leaking current from the membrane. To offer further clarification, each NoR is connected via an axoplasmic resistance in the circuit simulation. These connections have large resistances associated with them and thus allowed only an extremely small amount

of current through, producing the very small voltage values under 1 mV. It is also to be expected that all signals reach ground with enough time, allowing the capacitors to discharge their energy. The interesting aspect is that some capacitors discharged negatively from a positive voltage to reach ground, while many discharged positively from a negative voltage to reach ground. This resulted in sending back positive voltage values while the other locations were sending negative voltage values into the current module simulation.

4.3 Membrane Potentials

Positive discharging from a negative voltage to reach ground produced the visible deviations from an RC characteristic response most easily visible in Figure 29. Voltage measurements at NoRs five and seven shown in Figure 29 show a large "bump" deviation after the source is switched off. Without the boundary current source generating an induced current, the "bump," which details some form of discharged energy, must be due to the discharging of the capacitors. A discharging capacitor in line with the simulation and acting normally without the intervention of an outside element would not produce the result depicted in Figure 29. Voltage from the reverse discharging capacitors is the reason for this "bump".

Reverse discharging of the capacitors was not only responsible for the artifact of the "bump" but is also responsible for every RC exponential time characteristic element in the simulation results. Without any capacitive effects, each result would only exhibit a reduction of the signal in amplitude from the square wave pulse source. It is the capacitors in the simulation that are responsible for making the result more accurately

resemble the electrical characteristics of the human nervous membrane and represents the bulk of this work.

The result of this work also demonstrated a normal reduction in magnitude of the waveform as the signal was transmitted through a resistive media further away from the source. This has previously been explained but is again a result of the membrane potentials shown in Figure 29 appearing as they do because of the iterative solver utilized by COMSOL. The negative potential result seen in the electrical potential across the simulated nervous membrane was due to the same cause of a negative potential as previously explained. A difference does exist in the inverse "bump" found in the results of NoRs five and seven. It is the interaction of a reduction in magnitude and the negative values that produced this phenomenon. Without a large initial voltage, the signal can be more easily reduced from the surrounding tissues that reflect negative values of voltage. Surrounding tissues that reflect negative values of voltage also increase in their negativity because a large positive potential is lacking.

"Bumps" in the voltage plots, RC exponential time characteristic elements, and tissues that reflect negative values of voltage are all due to the nature of the simulation which meant that NoR6 was the most likely candidate for evaluation purposes because it was directly beneath the boundary current source. This advantageous placement allowed the NoR to most accurately portray the end goal of an RC characteristic expression of membrane potential. The final product of the simulation realized in the presentation of the membrane potential at NoR6 was not only qualitatively comparable to McNeal's derived response but also quantitatively comparable. Qualitatively the plots appear similar. Both climb at an exponential rise to a plateau and both similarly fall an

exponential decrease back to a plateau of zero volts. This is the desired RC characteristic response that McNeal presented and Szlavik adapted [26, 37]. Quantitatively the simulation results reach a value of around 10 mV with the results of this work being only slightly less than those of presented by McNeal in Figure 28 when using similar parameters in this simulation that were used in McNeal's work. A difference does exist though in the time domain. McNeal's work was performed over a span of 150 μ s whereas this work was performed over the course of 1000 μ s or 1 ms. A factor of ten is reasonably close to the results presented by McNeal. The reasoning behind the difference was that the SPICE simulator did not accurately portray the charging and discharging of the capacitor until an evaluation point of tenths of milliseconds was reached, which is larger than McNeal's pulse width. Before the pulse width of tenths of milliseconds was used, the simulator only produced square wave results, indicating the capacitor did not have adequate time to perform its function. Hopefully future work may discover a process by which the capacitor may be correctly simulated at small time intervals.

4.4 Future Work

Correctly simulating the time scale of membrane potential initiation is one of the most easily identifiable areas for improvement in this work. Besides improving the time scale, future iterations of this work might include adding more NoR which would better simulate the natural human membrane and provide more accurate results. This could be done by creating more circle geometries, applying terminal boundary conditions and adapting the SPICE netlist code to account for the larger number of nodes. Adding additional nodes of Ranvier is a relatively simple change. An even simpler change is to use the relative permittivity values that should have been applied to the original

geometry. Relative permittivity values decidedly did not significantly alter the simulation but applying the correct values to the simulation would better represent the real world case.

As improvements continue to develop, future implementation of this study should be able to better integrate software components such as the non-linear SPICE netlist code and COMSOL to better represent the nervous membrane characteristics. In addition, and perhaps more immediately, is the possibility of improving the geometry. Utilizing anatomical geometries that include more biological structures and correctly placed medical electrodes, instead of a rectangular geometry could provide a more robust model that more closely approximates the electrical signal propagation.

REFERENCES

1. Angel, Nathan. *Equivalent Circuit Implementation of Demyelinated Human Neuron in SPICE*. Thesis. San Luis Obispo: California Polytechnic State University, San Luis Obispo, 2011.
2. Barach, John Paul, Bradley J. Roth and Jr., John P. Wikswo. "Magnetic Measurements of Action Currents in a Single Nerve Axon: A Core-Conductor Model." *IEEE Transactions on Biomedical Engineering* BME-32 (1985): 136-140.
3. Belk, Jackie. *Structure and Function of the Neurologic System*. n.d.
<<http://www.studyblue.com/notes/note/n/structure-and-function-of-the-neurologic-system/deck/5119898>>.
4. Bodrich, T., H. Neubert and R. Disselnkötter. "Transient Finite Element Analysis of a SPICE-coupled Transformer with COMSOL Multiphysics." *COMSOL Conference 2010 Paris*. Paris: COMSOL Multiphysics, 2010.
5. Buschbacher, Ralph M. and Nathan D. Prahlow. *Manual of Nerve Conduction Studies*. New York, New York: Demos Medical Publishing, 2006.
6. Clark, John and Robert Plonsey. "A Mathematical Evaluation of the Core Conductor Model." *Biophysical Journal* 6 (1966): 95-112.
7. Clough, Ray W. and Edward L. Wilson. "Early Finite Element Research at Berkeley." *U.S. National Conference on Computational Mechanics*. 1999.
8. Clough, Ray W. "The finite element method in plane stress analysis." *ASCE Conference on Electronic Computation*. Pittsburgh, 1960.
9. COMSOL Multiphysics. *COMSOL Company*. 2014.
<<http://www.comsol.com/company>>.
10. —. *Model Gallery*. n.d. <<http://www.comsol.com/model/stresses-and-strains-in-a-wrench-8502>>.
11. Dorgan, Stephen J. and Richard B. Reilly. "A Model for Human Skin Impedance During Surface Functional Neuromuscular Stimulation." *IEEE Transactions on Rehabilitation Engineering* 7 (1999): 341-348.
12. Elert, Glenn. *Size of a Human: Body Proportions*. 2006. Hypertextbook.
<<http://hypertextbook.com/facts/2006/bodyproportions.shtml>>.

13. Elia, S., P. Lamberti and V. Tucci. "A Finite Element Model for The Axon of Nervous Cells." *COMSOL Conference 2009 Milan*. Milan, 2009.
14. Fry, Gordon. "Linear Cable Theory." *EECS 700 - Computational Neuroscience*. Information & Telecommunication Technology Center; The University of Kansas, n.d.
15. Furse, Cynthia, Douglas A. Christensen and Carl H. Durney. *Basic Introduction to Bioelectromagnetics*. 2. CRC Press, 2009.
<http://books.google.com/books?id=BrUrFMzXEJcC&pg=PA253&lpg=PA253&dq=appendix+a+electrical+properties+of+the+human+body&source=bl&ots=r2CDjiPHlm&sig=xSm31Acubcg2OY_loz6G8G6RRDI&hl=en&sa=X&ei=4GVYU8_HJ9i3yAS_yoG4Cw&ved=0CDoQ6AEwAg#v=onepage&q=appendix%20a%20>.
16. Goldman, L. and James S. Albus. "Computation of Impulse Conduction in Myelinated Fibers; Theoretical Basis of the Velocity-Diameter Relation." *Biophysical Journal* 8 (1968): 596-607.
17. Hall, Stephen S. Brain Pacemakers. Article. massachusetts: MIT Technology Review, 2001.
18. Hodgkin, A. L. and A. F. Huxley. "A Quantitative Description of Membrane Current and its Application to Conduction and Excitation in Nerve." *Journal of Physiology* 117 (1952): 500-544.
19. Huebner, Kenneth H., et al. *The Finite Element Mehtod for Engineers*. John Wiley & Sons, Inc., 2001.
20. Koch, Christof and Idan Segev. *Methods in Neuronal Modeling: From Ions to Networks*. Massachusetts: MIT Press, 1998.
21. Leuthardt, E C, et al. "The emerging world of motor neuroprosthetics: a neurosurgical perspective." *Neurosurgery* (2006): 1-14.
22. Lussier, J. J. and W. A. H. Rushton. "The excitability of a single fibre in a nerve trunk." *The Journal of Physiology* 117 (1952): 87-108.
23. lvs-biology. *Wikispaces Classroom*. n.d. <<http://lvs-biology.wikispaces.com/Nervous+system>>.
24. Marieb, Elaine N. and Katja Hoehn. *Human Anatomy & Physiology*. 7. San Fransisco: Pearson Education, Inc., 2007.

25. Martinek, Johannes, et al. "A Novel Approach to Simulate Hodgkin-Huxley-like Excitation With COMSOL Multiphysics." *Artificial Organs* 32 (2008): 614-619.
26. McNeal, Donald R. "Analysis of a Model for Excitation of Myelinated Nerve." *IEEE Transactions on Biomedical Engineering* BME-23 (1976): 329-337.
27. Miklavcic, Damijan, Natasa Pavselj and Francis X. Hart. "Electric Properties of Tissues." Akay, Metin. *Wiley Encyclopedia of Biomedical Engineering*. Wiley-Interscience, 2006.
28. Miller, Robert F. *Linear Electrical Circuit Theory*. Lecture. Minneapolis: University of Minnesota, Department of Neuroscience, 2006.
29. Nagel, L. W. and D. O. Pederson. "SPICE (Simulation Program with Integrated Circuit Emphasis)." *Memorandum No. ERL-M382*. Berkeley: Electronics Research Laboratory College of Engineering University of California, Berkeley, 12 April 1973. Memorandum.
30. Offner, Franklin, Alvin Weinberg and Gale Young. "Nerve conduction theory: Some mathematical consequences of Bernstein's model." *The bulletin of mathematical biophysics* (1940): 89-103.
31. Rushton, W. A. H. "The effect upon the threshold for nervous excitation of the length of nerve exposed, and the angle between current and nerve." *The Journal of Physiology* 63 (1927): 357-377.
32. Schell, Kathleen A. and Julie Keith Waterhouse. "Comparison of Forearm and Upper Arm: Automatic, Noninvasive Blood Pressures in College Students." *The Internet Journal of Advanced Nursing Practice* 9 (n.d.).
33. Shatin, D, K Mullett and G Hulst. "Totally implantable spinal cord stimulation for chronic pain: design and efficacy." *Pacing Clin Electrophysiol* (1986): 577-583.
34. Society for Industrial and Applied Mathematics. "Obituary: Germund Dahlquist." *SIAM News*. Vol. 38. Philadelphia: Society for Industrial and Applied Mathematics, May 2005.
35. Soto, Nathan Daniel. *Characterizing Nerve Fiber Activation by Varying Fiber Diameter and Depth Within a Conductive Medium: A Finite Element Approach*. Thesis. San Luis Obispo: California Polytechnic State University, San Luis Obispo, 2011.
36. Szlavik, R. B. and G. E. Turner. "A novel method for characterization of peripheral nerve fiber size distributions by group delay measurements and simulated annealing optimization." *Annual International Conference of the IEEE*

Engineering in Medicine and Biology Society. IEEE Engineering in Medicine and Biology Society, 2008. 5008-5014.

37. Szlavik, Robert B. and Hubert de Bruin. "The effect of stimulus current pulse width on nerve fiber size recruitment patterns." *Medical Engineering & Physics* 21 (1999): 507-515.
38. Theory of Knowledge. 6.5 *Nerves, hormones and homeostasis*. n.d.
<http://www.tokresource.org/tok_classes/biobiobio/biomenu/nerves_hormones_homeostasis/index.htm>.
39. Timofeeva, Yulia. "Single Neuron Models." Lecture. 2008.
40. Tsui, Ban C.H. "Electrical Nerve Stimulation." Chan, Vincent. *Atlas of Ultrasound- and Nerve Stimulation- Guided Regional Anesthesia*. 2008. Springer, 2007. 9-18.
41. Weiss, Thomas Fischer. *Cellular Biophysics*. Massachusetts: Massachusetts Institute of Technology, 1996.
42. Wolfer, Skye. *DOS PSpice Helps*. n.d. Brigham Young University.
<http://vlsi.groups.et.byu.net/download/pspice_tutorial/dos_ps/dos_ps.html>.
43. Young, Eric. *Systems Biology II: Neural Systems Lecture 8, Linear Cable Theory*. Lecture. Baltimore: Johns Hopkins University, n.d.
44. —. *Systems Biology II: Neural Systems Lecture 9, Nonlinear Cable Theory*. Lecture. Baltimore: Johns Hopkins University, n.d.

APPENDICES

Appendix A: Non-Linear SPICE Netlist Code

* Full Code For Input Into COMSOL

.OPTIONS NUMDGT=6

* Cell Length (m)

.PARAM LENGTH={(80.0E-6)*100}

* Cell Radius (m)

.PARAM RADIUS={(10.0E-6)*100}

* Injected Current Magnitude Per Unit Area (A/cm²)

.PARAM AMPL=0.01

* Math Constant

.PARAM PIE=3.14159

* Calculated Stimulus Current Amplitude (A)

.PARAM STIMAMP={(2*PIE*RADIUS*LENGTH + 2*PIE*RADIUS^2)*AMPL}

I1 0 1 pulse(0 {STIMAMP} 10E-3 100E-9 100E-9 0.1E-3 0)

*pulse(0 6E-9 10E-3 100.0E-9 100.0E-9 .1E-3 0)

RD 1 0 1.0E10

xsub 1 0 NEURON

*Code Below Used To Be A Subcircuit But To Import To COMSOL

*Turned The Subcircuit Into Part Of The Circuit Code

*

*

*

.SUBCKT NEURON 31 30

.PARAM CAPPUA=10.0E-7

*

*

* coNa = 491.0E-3 Extracellular sodium concentration (mol/L)

* ciNa = 50.0E-3 Intracellular sodium concentration (mol/L)

* coK = 20.11E-3 Extracellular potassium concentration
(mol/L)

* ciK = 400.0E-3 Intracellular potassium concentration
(mol/L)


```

*

*   GNaMax=120.0E-3

*   GKMax =36.0E-3

*

*   V_r    = -62.5E-3           Resting Membrane Potential (V)

*

*   Temp   = 6.3                Temperature (Degrees Celsius)

*

*   b              = 0.02       Relative permeability of sodium to
potassium

*   R              = 8.314       Reiberg gas constant
(joules/(mole*kelvin))

*   Z              = 1.0        Sodium and potassium ionic
valence

*   F              = 9.648E4     Faraday's constant (coulombs/mole)

*

*****

*

.PARAM MO=0.0393

.PARAM HO=0.6798

.PARAM NO=0.2803

```

.PARAM VNA=55.0E-3

.PARAM VK=-72.0E-3

*

* CALCULATED PARAMETERS

.PARAM CELCAP={ (2*PIE*RADIUS*LENGTH + 2*PIE*RADIUS^2)*CAPPUA }

*

*

*

*This Portion Had To Be Reorganized To Suite COMSOL

VINA 20 0 0

VNA 11 0 {VNA}

RNA 11 0 1E10

VIK 21 0 0

VK 12 0 {VK}

*

*

*

FNA 31 27 VINA 1

FK 31 28 VIK 1

VNk 28 30 {VK}

VNNa 27 30 {VNA}

ENAK 26 0 31 30 1

CE 31 30 {CELCAP} IC=-62.5E-3

*Sodium current current pathway

*M variable

CM 2 0 0.26E-3 IC={MO}

RM 2 0 1E10

GAM 0 2 POLY(2) 2 0 5 0 0 0 1 0 -1

GBM 0 2 POLY(2) 2 0 6 0 0 0 0 0 -1

EAM 5 0 value={-0.1*(v(26)*1E3+35)/(exp(-0.1*(v(26)*1E3+35))-1)}

RAM 5 0 1E10

EBM 6 0 value={4*exp(-(v(26)*1E3+60)/18)}

RBM 6 0 1E10

* Sodium current current pathway

* H Variable

CH 3 0 0.26E-3 IC={HO}

RH 3 0 1E10

GAH 0 3 POLY(2) 3 0 7 0 0 0 1 0 -1

GBH 0 3 POLY(2) 3 0 8 0 0 0 0 0 -1

EAH 7 0 value={0.07*exp(-0.05*(v(26)*1E3+60))}

RAH 7 0 1E10

EBH 8 0 value={1/(1+exp(-0.1*(v(26)*1E3+30)))}

RBH 8 0 1E10

*Potassium current current pathway

* K parameters

CN 4 0 0.26E-3 IC={NO}

RN 4 0 1E10

GAN 0 4 POLY(2) 4 0 9 0 0 0 1 0 -1

GBN 0 4 POLY(2) 4 0 10 0 0 0 0 0 -1

EAN 9 0 value={-0.01*(v(26)*1E3+50)/(exp(-0.1*(v(26)*1E3+50))-1)}

RAN 9 0 1E10

EBN 10 0 value={0.125*exp(-0.0125*(v(26)*1E3+60))}

RBN 10 0 1E10

EMNA 15 0 26 11 1

RMNA 15 0 1E10

EM3 53 0 POLY(1) 2 0 0 0 0 1

EM3H 16 0 POLY(2) 53 0 3 0 0 0 0 0 1

RM3H 16 0 1E10

GNA 0 20 POLY(2) 15 0 16 0 0 0 0 0 6.7858E-006

RK 12 0 1E10

EMK 17 0 26 12 1

RMK 17 0 1E10

EN4 18 0 poly(1) 4 0 0 0 0 1

RN4 18 0 1E10

GK 0 21 POLY(2) 17 0 18 0 0 0 0 0 2.0358E-006

.ENDS

*

*

*

.tran 20.0E-6 20E-3 0 1E-6

.probe

.print TRAN V(1)

.END

Appendix B: Linear SPICE Netlist Code

* Myelinated axon equivalent circuit modeling with voltage sources

* Fiber Diameter (m)

* Pulled From Figure in Szlavik Paper

.PARAM FIBERDIA=0.00002

* Cytoplasm Resistivity (ohm-m)

.PARAM CYTORES=1.1

* Membrane Conductance (S/m²)

.PARAM MEMCOND=304

* Membrane Capacitance (F/m²)

.PARAM MEMCAP=0.02

* Node of Ranvier Width (um)

.PARAM NODEWIDTH=0.0000025

* Ratio of axon to fiber radius

.PARAM AFRATIO=0.7

*Current Source Parameter (A)

.PARAM CURRENTSOURCE=0.015

* Axon Diameter (m)

.PARAM AXONDIA={ AFRATIO*FIBERDIA }

* Fiber Radius (m)

.PARAM FIBERRADIUS={ (0.5*FIBERDIA) }

* Axon Radius (m)

.PARAM AXONRADIUS={ (0.5*AXONDIA) }

* Node of Ranvier Spacing (m)

.PARAM NODESPACE={ 100*FIBERDIA }

* Equivalent Axoplasm Resistance (ohm)

.PARAM

EAXORES={ (CYTORES*NODESPACE)/(3.14159265359*(AXONRADIUS^2)) }

* Equivalent Membrane Resistance (ohm)

.PARAM

EMEMRES={ 1/(2*3.14159265359*MEMCOND*AXONRADIUS*NODEWIDTH) }

* Equivalent Membrane Capacitance (F)

.PARAM

EMEMCAP={ (2*3.14159265359*MEMCAP*AXONRADIUS*NODEWIDTH) }

* Calculation of Controlled Sources Gain Done in Accompanying Excel

*Connecting COMSOL nodes into circuit for Nodes of Ranvier

X1 1 2 3 4 5 6 7 8 9 10 11 NoRs

*Connecting COMSOL nodes into circuit for Source and Ground Electrodes

X2 1000 0 Electrodes

*Current Source for COMSOL Simulation


```
*V1 1000 0 pulse(0      0.1      0      0.00000001 0.00000001 0.0005
0.001)
```

```
*V + - pulse(initialvoltage pulsedvoltage delay falltime risetime
pulsewidth period)
```

*Beginning Resistance Representing Myelinated Axoplasm

```
RA0 0 101 14291464.28
```

*Node of Ranvier 1

```
R1 1 101 29916342.69      ;Membrane Resistance
```

```
C1 1 101 0.00000000000219911485751286      ;Membrane Capacitance
```

*Axoplasm Resistance 1

```
RA1 101 102 14291464.28
```

*Node of Ranvier 2

```
R2 2 102 29916342.69      ;Membrane Resistance
```

```
C2 2 102 0.00000000000219911485751286      ;Membrane Capacitance
```

*Axoplasm Resistance 2

```
RA2 102 103 14291464.28
```

*Node of Ranvier 3

R3 3 103 29916342.69 ;Membrane Resistance

C3 3 103 0.00000000000219911485751286 ;Membrane Capacitance

*Axoplasm Resistance 3

RA3 103 104 14291464.28

*Node of Ranvier 4

R4 4 104 29916342.69 ;Membrane Resistance

C4 4 104 0.00000000000219911485751286 ;Membrane Capacitance

*Axoplasm Resistance 4

RA4 104 105 14291464.28

*Node of Ranvier 5

R5 5 105 29916342.69 ;Membrane Resistance

C5 5 105 0.00000000000219911485751286 ;Membrane Capacitance

*Axoplasm Resistance 5

RA5 105 106 14291464.28

*Node of Ranvier 6

R6 6 106 29916342.69 ;Membrane Resistance

C6 6 106 0.00000000000219911485751286 ;Membrane Capacitance

*Axoplasm Resistance 6

RA6 106 107 14291464.28

*Node of Ranvier 7

R7 7 107 29916342.69 ;Membrane Resistance

C7 7 107 0.00000000000219911485751286 ;Membrane Capacitance

*Axoplasm Resistance 7

RA7 107 108 14291464.28

*Node of Ranvier 8

R8 8 108 29916342.69 ;Membrane Resistance

C8 8 108 0.00000000000219911485751286 ;Membrane Capacitance

*Axoplasm Resistance 8

RA8 108 109 14291464.28

*Node of Ranvier 9

R9 9 109 29916342.69 ;Membrane Resistance

C9 9 109 0.00000000000219911485751286 ;Membrane Capacitance

*Axoplasm Resistance 9

RA9 10 110 14291464.28

*Node of Ranvier 10

R10 10 110 29916342.69 ;Membrane Resistance

C10 10 110 0.00000000000219911485751286 ;Membrane Capacitance

*Axoplasm Resistance 10

RA10 110 111 14291464.28

*Node of Ranvier 11

R11 11 111 29916342.69 ;Membrane Resistance

C11 11 111 0.00000000000219911485751286 ;Membrane Capacitance

*Ending Resistance Representing Myelinated Axoplasm

RA11 111 0 14291464.28

*Transmitting Voltage Back into COMSOL

E1 201 0 1 101 1

E2 202 0 2 102 1

E3 203 0 3 103 1

E4 204 0 4 104 1

E5 205 0 5 105 1

E6 206 0 6 106 1

E7 207 0 7 107 1

E8 208 0 8 108 1

E9 209 0 9 109 1

E10 210 0 10 110 1

E11 211 0 11 111 1

RT1 201 0 1

RT2 202 0 1

RT3 203 0 1

RT4 204 0 1

RT5 205 0 1

RT6 206 0 1

RT7 207 0 1

RT8 208 0 1

RT9 209 0 1

RT10 210 0 1

RT11 211 0 1

*Connection to COMSOL

*	NoR1	NoR2	NoR3	NoR4	NoR5	NoR6	NoR7
---	------	------	------	------	------	------	------

NoR8	NoR9	NoR10	NoR11
------	------	-------	-------

```
.SUBCKT NoRs      NoRone  NoRtwo  NoRthree  NoRfour  NoRfive  NoRsix  
NoRseven  NoReight  NoRnine  NoRten  NoReleven  COMSOL: *
```

```
.ENDS
```

```
*          Source      Ground
```

```
.SUBCKT Electrodes sourcenode  groundnode  COMSOL: *
```

```
.ENDS
```

```
.TRAN 0.0001 0.001
```

```
.PROBE
```

Appendix C: COMSOL Solver Log

Step	Time	Stepsize	Res	Jac	Sol	Order	Tfail	NLfail
0	0		2	3	2			0
1	3.9062e-009	3.9062e-009	11	8	11	1	4	0
2	5.8594e-009	1.9531e-009	14	10	14	1	5	0
3	9.7656e-009	3.9062e-009	15	11	15	1	5	0
4	9.8877e-009	1.2207e-010	22	15	22	1	8	0
5	9.9487e-009	6.1035e-011	25	17	25	1	9	0
6	9.9792e-009	3.0518e-011	28	19	28	1	10	0
7	9.9945e-009	1.5259e-011	31	21	31	1	11	0
8	9.9964e-009	1.9073e-012	36	24	36	1	13	0
9	9.9974e-009	9.5367e-013	39	26	39	1	14	0
10	9.9993e-009	1.9073e-012	40	27	40	1	14	0
11	9.9995e-009	2.3842e-013	45	30	45	1	16	0
12	1e-008	4.7684e-013	46	31	46	1	16	0
13	1e-008	3.7253e-015	55	36	55	1	20	0
14	1e-008	1.8626e-015	58	38	58	1	21	0
15	1e-008	3.7253e-015	59	39	59	1	21	0
16	1e-008	4.6566e-016	65	42	65	1	23	0
17	1e-008	1.0962e-016	73	44	73	1	24	0
18	1e-008	1.0962e-016	74	44	74	1	24	0
19	1e-008	9.8658e-017	76	44	76	1	24	0
20	1e-008	9.8658e-017	77	44	77	1	24	0
21	1e-008	8.8792e-017	79	44	79	1	24	0
22	1e-008	8.8792e-017	81	44	81	1	24	0
23	1e-008	8.8792e-017	83	44	83	1	24	0
24	1e-008	1.7758e-016	85	44	85	2	24	0
25	1e-008	1.7758e-016	86	44	86	2	24	0
26	1e-008	1.7758e-016	87	44	87	2	24	0
27	1e-008	3.5517e-016	89	45	89	2	24	0
28	1e-008	7.1034e-016	91	46	91	2	24	0
29	1e-008	7.1034e-016	92	46	92	2	24	0
30	1e-008	1.4207e-015	94	47	94	2	24	0
31	1e-008	1.4207e-015	95	47	95	2	24	0
32	1e-008	1.4207e-015	96	47	96	2	24	0
33	1e-008	2.8414e-015	98	48	98	2	24	0
34	1e-008	2.8414e-015	99	48	99	2	24	0
35	1e-008	2.8414e-015	100	48	100	2	24	0
36	1e-008	2.8414e-015	101	48	101	2	24	0
37	1e-008	5.6827e-015	103	48	103	3	24	0
38	1e-008	5.6827e-015	104	48	104	3	24	0
39	1e-008	1.1365e-014	106	49	106	3	24	0
40	1e-008	1.1365e-014	107	49	107	3	24	0
41	1e-008	1.1365e-014	108	49	108	3	24	0
42	1e-008	1.1365e-014	109	49	109	3	24	0
43	1e-008	1.1365e-014	110	49	110	3	24	0
44	1e-008	2.2731e-014	112	50	112	4	24	0
45	1e-008	2.2731e-014	113	50	113	4	24	0
46	1e-008	2.9406e-014	117	51	117	4	25	0
47	1e-008	2.9406e-014	119	51	119	4	25	0
48	1e-008	2.9406e-014	120	51	120	4	25	0
49	1e-008	2.9406e-014	122	51	122	4	25	0
50	1e-008	2.9406e-014	123	51	123	4	25	0
51	1e-008	2.9406e-014	124	51	124	4	25	0

52	1e-008	5.8812e-014	126	51	126	4	25	0
53	1e-008	5.8812e-014	128	51	128	3	25	0
54	1e-008	5.8812e-014	129	51	129	3	25	0
55	1.0001e-008	3.6231e-014	134	51	134	3	26	0
56	1.0001e-008	3.6231e-014	135	51	135	3	26	0
57	1.0001e-008	3.6231e-014	136	51	136	3	26	0
58	1.0001e-008	3.2608e-014	138	51	138	3	26	0
59	1.0001e-008	3.2608e-014	139	51	139	3	26	0
60	1.0001e-008	3.2608e-014	140	51	140	3	26	0
61	1.0001e-008	3.2608e-014	141	51	141	3	26	0
62	1.0001e-008	5.8695e-014	145	52	145	2	27	0
63	1.0001e-008	5.8695e-014	146	52	146	2	27	0
64	1.0001e-008	5.8695e-014	147	52	147	2	27	0
65	1.0001e-008	5.8695e-014	148	52	148	2	27	0
66	1.0001e-008	1.1739e-013	150	52	150	3	27	0
67	1.0001e-008	1.1739e-013	151	52	151	3	27	0
68	1.0001e-008	1.1739e-013	152	52	152	3	27	0
69	1.0001e-008	1.1739e-013	153	52	153	3	27	0
70	1.0002e-008	1.1739e-013	154	52	154	3	27	0
71	1.0002e-008	2.3478e-013	156	53	156	2	27	0
72	1.0002e-008	2.3478e-013	157	53	157	2	27	0
73	1.0002e-008	2.3478e-013	158	53	158	2	27	0
74	1.0002e-008	2.3478e-013	159	53	159	2	27	0
75	1.0003e-008	2.3478e-013	161	53	161	3	27	0
76	1.0003e-008	4.6956e-013	163	53	163	3	27	0
77	1.0004e-008	4.6956e-013	164	53	164	3	27	0
78	1.0004e-008	4.6956e-013	165	53	165	3	27	0
79	1.0005e-008	4.6956e-013	166	53	166	3	27	0
80	1.0005e-008	4.6956e-013	167	53	167	3	27	0
81	1.0006e-008	9.3912e-013	169	54	169	3	27	0
82	1.0007e-008	9.3912e-013	170	54	170	3	27	0
83	1.0008e-008	9.3912e-013	171	54	171	3	27	0
84	1.001e-008	1.8782e-012	173	55	173	3	27	0
85	1.0012e-008	1.8782e-012	174	55	174	3	27	0
86	1.0014e-008	1.8782e-012	175	55	175	3	27	0
87	1.0015e-008	1.8782e-012	176	55	176	3	27	0
88	1.0017e-008	1.8782e-012	177	55	177	3	27	0
89	1.0021e-008	3.7565e-012	179	56	179	4	27	0
90	1.0025e-008	3.7565e-012	180	56	180	4	27	0
91	1.003e-008	4.7479e-012	184	57	184	3	28	0
92	1.0034e-008	4.7479e-012	186	57	186	3	28	0
93	1.0039e-008	4.7479e-012	188	57	188	3	28	0
94	1.0044e-008	4.7479e-012	190	57	190	3	28	0
95	1.0049e-008	4.7479e-012	191	57	191	3	28	0
96	1.0057e-008	8.5462e-012	195	57	195	3	29	0
97	1.0066e-008	8.5462e-012	196	57	196	3	29	0
98	1.0074e-008	8.5462e-012	197	57	197	3	29	0
99	1.0083e-008	8.5462e-012	199	57	199	2	29	0
100	1.0096e-008	1.3117e-011	203	58	203	1	30	0
101	1.0107e-008	1.1415e-011	205	58	205	1	30	0
102	1.013e-008	2.283e-011	207	59	207	1	30	0
103	1.0153e-008	2.283e-011	208	59	208	1	30	0
104	1.0199e-008	4.566e-011	210	60	210	1	30	0
105	1.0244e-008	4.566e-011	211	60	211	1	30	0
106	1.0336e-008	9.132e-011	213	61	213	1	30	0

107	1.0427e-008	9.132e-011	214	61	214	1	30	0
108	1.061e-008	1.8264e-010	216	62	216	1	30	0
109	1.0975e-008	3.6528e-010	218	63	218	1	30	0
110	1.1705e-008	7.3056e-010	220	64	220	1	30	0
111	1.3166e-008	1.4611e-009	221	65	221	1	30	0
112	1.6089e-008	2.9222e-009	222	66	222	1	30	0
113	2.1933e-008	5.8445e-009	223	67	223	1	30	0
114	3.3622e-008	1.1689e-008	224	68	224	1	30	0
115	5.7e-008	2.3378e-008	225	69	225	1	30	0
116	1.0376e-007	4.6756e-008	226	70	226	1	30	0
117	1.9727e-007	9.3512e-008	227	71	227	1	30	0
118	3.8429e-007	1.8702e-007	229	72	229	1	30	0
119	7.5834e-007	3.7405e-007	231	73	231	1	30	0
	1e-006	- out						
120	1.5064e-006	7.481e-007	233	74	233	1	30	0
	2e-006	- out						
121	2.2545e-006	7.481e-007	234	74	234	1	30	0
	3e-006	- out						
122	3.0026e-006	7.481e-007	235	74	235	1	30	0
	4e-006	- out						
123	4.4988e-006	1.4962e-006	237	74	237	2	30	0
	5e-006	- out						
124	5.995e-006	1.4962e-006	238	74	238	2	30	0
	6e-006	- out						
	7e-006	- out						
	8e-006	- out						
125	8.9874e-006	2.9924e-006	240	75	240	2	30	0
	9e-006	- out						
	1e-005	- out						
	1.1e-005	- out						
126	1.198e-005	2.9924e-006	241	75	241	2	30	0
	1.2e-005	- out						
	1.3e-005	- out						
	1.4e-005	- out						
127	1.4972e-005	2.9924e-006	242	75	242	2	30	0
	1.5e-005	- out						
	1.6e-005	- out						
	1.7e-005	- out						
128	1.7965e-005	2.9924e-006	243	75	243	2	30	0
	1.8e-005	- out						
	1.9e-005	- out						
	2e-005	- out						
	2.1e-005	- out						
	2.2e-005	- out						
	2.3e-005	- out						
129	2.3949e-005	5.9848e-006	245	75	245	3	30	0
	2.4e-005	- out						
	2.5e-005	- out						
	2.6e-005	- out						
	2.7e-005	- out						
	2.8e-005	- out						
	2.9e-005	- out						
130	2.9336e-005	5.3863e-006	247	75	247	3	30	0
	3e-005	- out						
	3.1e-005	- out						

	3.2e-005	- out						
	3.3e-005	- out						
	3.4e-005	- out						
131	3.4722e-005	5.3863e-006	248	75	248	3	30	0
	3.5e-005	- out						
	3.6e-005	- out						
	3.7e-005	- out						
	3.8e-005	- out						
	3.9e-005	- out						
	4e-005	- out						
132	4.0108e-005	5.3863e-006	249	75	249	3	30	0
	4.1e-005	- out						
	4.2e-005	- out						
	4.3e-005	- out						
	4.4e-005	- out						
	4.5e-005	- out						
133	4.5494e-005	5.3863e-006	250	75	250	3	30	0
	4.6e-005	- out						
	4.7e-005	- out						
	4.8e-005	- out						
	4.9e-005	- out						
	5e-005	- out						
134	5.0881e-005	5.3863e-006	251	75	251	3	30	0
	5.1e-005	- out						
	5.2e-005	- out						
	5.3e-005	- out						
	5.4e-005	- out						
	5.5e-005	- out						
	5.6e-005	- out						
	5.7e-005	- out						
	5.8e-005	- out						
	5.9e-005	- out						
	6e-005	- out						
	6.1e-005	- out						
135	6.1653e-005	1.0773e-005	253	76	253	3	30	0
	6.2e-005	- out						
	6.3e-005	- out						
	6.4e-005	- out						
	6.5e-005	- out						
	6.6e-005	- out						
	6.7e-005	- out						
	6.8e-005	- out						
	6.9e-005	- out						
	7e-005	- out						
	7.1e-005	- out						
136	7.1349e-005	9.6953e-006	255	76	255	3	30	0
	7.2e-005	- out						
	7.3e-005	- out						
	7.4e-005	- out						
	7.5e-005	- out						
	7.6e-005	- out						
	7.7e-005	- out						
	7.8e-005	- out						
	7.9e-005	- out						
	8e-005	- out						

	8.1e-005	- out						
137	8.1044e-005	9.6953e-006	256	76	256	3	30	0
	8.2e-005	- out						
	8.3e-005	- out						
	8.4e-005	- out						
	8.5e-005	- out						
	8.6e-005	- out						
	8.7e-005	- out						
	8.8e-005	- out						
	8.9e-005	- out						
	9e-005	- out						
138	9.0739e-005	9.6953e-006	257	76	257	3	30	0
	9.1e-005	- out						
	9.2e-005	- out						
	9.3e-005	- out						
	9.4e-005	- out						
	9.5e-005	- out						
	9.6e-005	- out						
	9.7e-005	- out						
	9.8e-005	- out						
	9.9e-005	- out						
	0.0001	- out						
139	0.00010043	9.6953e-006	258	76	258	3	30	0
	0.000101	- out						
	0.000102	- out						
	0.000103	- out						
	0.000104	- out						
	0.000105	- out						
	0.000106	- out						
	0.000107	- out						
	0.000108	- out						
	0.000109	- out						
	0.00011	- out						
140	0.00011013	9.6953e-006	259	76	259	3	30	0
	0.000111	- out						
	0.000112	- out						
	0.000113	- out						
	0.000114	- out						
	0.000115	- out						
	0.000116	- out						
	0.000117	- out						
	0.000118	- out						
	0.000119	- out						
	0.00012	- out						
	0.000121	- out						
	0.000122	- out						
	0.000123	- out						
	0.000124	- out						
	0.000125	- out						
	0.000126	- out						
	0.000127	- out						
	0.000128	- out						
	0.000129	- out						
141	0.00012952	1.9391e-005	261	77	261	3	30	0
	0.00013	- out						

	0.000131		-	out					
	0.000132		-	out					
	0.000133		-	out					
	0.000134		-	out					
	0.000135		-	out					
	0.000136		-	out					
	0.000137		-	out					
	0.000138		-	out					
	0.000139		-	out					
	0.00014		-	out					
	0.000141		-	out					
	0.000142		-	out					
	0.000143		-	out					
	0.000144		-	out					
	0.000145		-	out					
	0.000146		-	out					
	0.000147		-	out					
	0.000148		-	out					
142	0.00014891	1.9391e-005	262	77	262	3	30	0	
	0.000149		-	out					
	0.00015		-	out					
	0.000151		-	out					
	0.000152		-	out					
	0.000153		-	out					
	0.000154		-	out					
	0.000155		-	out					
	0.000156		-	out					
	0.000157		-	out					
	0.000158		-	out					
	0.000159		-	out					
	0.00016		-	out					
	0.000161		-	out					
	0.000162		-	out					
	0.000163		-	out					
	0.000164		-	out					
	0.000165		-	out					
	0.000166		-	out					
	0.000167		-	out					
	0.000168		-	out					
143	0.0001683	1.9391e-005	263	77	263	3	30	0	
	0.000169		-	out					
	0.00017		-	out					
	0.000171		-	out					
	0.000172		-	out					
	0.000173		-	out					
	0.000174		-	out					
	0.000175		-	out					
	0.000176		-	out					
	0.000177		-	out					
	0.000178		-	out					
	0.000179		-	out					
	0.00018		-	out					
	0.000181		-	out					
	0.000182		-	out					
	0.000183		-	out					

	0.000184	- out						
	0.000185	- out						
	0.000186	- out						
	0.000187	- out						
144	0.00018769	1.9391e-005	264	77	264	3	30	0
	0.000188	- out						
	0.000189	- out						
	0.00019	- out						
	0.000191	- out						
	0.000192	- out						
	0.000193	- out						
	0.000194	- out						
	0.000195	- out						
	0.000196	- out						
	0.000197	- out						
	0.000198	- out						
	0.000199	- out						
	0.0002	- out						
	0.000201	- out						
	0.000202	- out						
	0.000203	- out						
	0.000204	- out						
	0.000205	- out						
	0.000206	- out						
	0.000207	- out						
145	0.00020708	1.9391e-005	265	77	265	3	30	0
	0.000208	- out						
	0.000209	- out						
	0.00021	- out						
	0.000211	- out						
	0.000212	- out						
	0.000213	- out						
	0.000214	- out						
	0.000215	- out						
	0.000216	- out						
	0.000217	- out						
	0.000218	- out						
	0.000219	- out						
	0.00022	- out						
	0.000221	- out						
	0.000222	- out						
	0.000223	- out						
	0.000224	- out						
	0.000225	- out						
	0.000226	- out						
146	0.00022647	1.9391e-005	267	77	267	4	30	0
	0.000227	- out						
	0.000228	- out						
	0.000229	- out						
	0.00023	- out						
	0.000231	- out						
	0.000232	- out						
	0.000233	- out						
	0.000234	- out						
	0.000235	- out						

	0.000236		- out						
	0.000237		- out						
	0.000238		- out						
	0.000239		- out						
	0.00024		- out						
	0.000241		- out						
	0.000242		- out						
	0.000243		- out						
	0.000244		- out						
	0.000245		- out						
	0.000246		- out						
	0.000247		- out						
	0.000248		- out						
	0.000249		- out						
	0.00025		- out						
	0.000251		- out						
	0.000252		- out						
	0.000253		- out						
	0.000254		- out						
	0.000255		- out						
	0.000256		- out						
	0.000257		- out						
	0.000258		- out						
	0.000259		- out						
	0.00026		- out						
	0.000261		- out						
	0.000262		- out						
	0.000263		- out						
	0.000264		- out						
	0.000265		- out						
147	0.00026525	3.8781e-005		269	78	269	4	30	0
	0.000266		- out						
	0.000267		- out						
	0.000268		- out						
	0.000269		- out						
	0.00027		- out						
	0.000271		- out						
	0.000272		- out						
	0.000273		- out						
	0.000274		- out						
	0.000275		- out						
	0.000276		- out						
	0.000277		- out						
	0.000278		- out						
	0.000279		- out						
	0.00028		- out						
	0.000281		- out						
	0.000282		- out						
	0.000283		- out						
	0.000284		- out						
	0.000285		- out						
	0.000286		- out						
	0.000287		- out						
	0.000288		- out						
	0.000289		- out						

	0.00029	- out						
	0.000291	- out						
	0.000292	- out						
	0.000293	- out						
	0.000294	- out						
	0.000295	- out						
	0.000296	- out						
	0.000297	- out						
	0.000298	- out						
	0.000299	- out						
	0.0003	- out						
	0.000301	- out						
	0.000302	- out						
	0.000303	- out						
	0.000304	- out						
148	0.00030404	3.8781e-005	270	78	270	4	30	0
	0.000305	- out						
	0.000306	- out						
	0.000307	- out						
	0.000308	- out						
	0.000309	- out						
	0.00031	- out						
	0.000311	- out						
	0.000312	- out						
	0.000313	- out						
	0.000314	- out						
	0.000315	- out						
	0.000316	- out						
	0.000317	- out						
	0.000318	- out						
	0.000319	- out						
	0.00032	- out						
	0.000321	- out						
	0.000322	- out						
	0.000323	- out						
	0.000324	- out						
	0.000325	- out						
	0.000326	- out						
	0.000327	- out						
	0.000328	- out						
	0.000329	- out						
	0.00033	- out						
	0.000331	- out						
	0.000332	- out						
	0.000333	- out						
	0.000334	- out						
	0.000335	- out						
	0.000336	- out						
	0.000337	- out						
	0.000338	- out						
	0.000339	- out						
	0.00034	- out						
	0.000341	- out						
	0.000342	- out						
149	0.00034282	3.8781e-005	271	78	271	4	30	0

	0.000343	- out						
	0.000344	- out						
	0.000345	- out						
	0.000346	- out						
	0.000347	- out						
	0.000348	- out						
	0.000349	- out						
	0.00035	- out						
	0.000351	- out						
	0.000352	- out						
	0.000353	- out						
	0.000354	- out						
	0.000355	- out						
	0.000356	- out						
	0.000357	- out						
	0.000358	- out						
	0.000359	- out						
	0.00036	- out						
	0.000361	- out						
	0.000362	- out						
	0.000363	- out						
	0.000364	- out						
	0.000365	- out						
	0.000366	- out						
	0.000367	- out						
	0.000368	- out						
	0.000369	- out						
	0.00037	- out						
	0.000371	- out						
	0.000372	- out						
	0.000373	- out						
	0.000374	- out						
	0.000375	- out						
	0.000376	- out						
	0.000377	- out						
	0.000378	- out						
	0.000379	- out						
	0.00038	- out						
	0.000381	- out						
150	0.0003816	3.8781e-005	273	78	273	3	30	0
	0.000382	- out						
	0.000383	- out						
	0.000384	- out						
	0.000385	- out						
	0.000386	- out						
	0.000387	- out						
	0.000388	- out						
	0.000389	- out						
	0.00039	- out						
	0.000391	- out						
	0.000392	- out						
	0.000393	- out						
	0.000394	- out						
	0.000395	- out						
	0.000396	- out						

0.000397	- out
0.000398	- out
0.000399	- out
0.0004	- out
0.000401	- out
0.000402	- out
0.000403	- out
0.000404	- out
0.000405	- out
0.000406	- out
0.000407	- out
0.000408	- out
0.000409	- out
0.00041	- out
0.000411	- out
0.000412	- out
0.000413	- out
0.000414	- out
0.000415	- out
0.000416	- out
0.000417	- out
0.000418	- out
0.000419	- out
0.00042	- out
0.000421	- out
0.000422	- out
0.000423	- out
0.000424	- out
0.000425	- out
0.000426	- out
0.000427	- out
0.000428	- out
0.000429	- out
0.00043	- out
0.000431	- out
0.000432	- out
0.000433	- out
0.000434	- out
0.000435	- out
0.000436	- out
0.000437	- out
0.000438	- out
0.000439	- out
0.00044	- out
0.000441	- out
0.000442	- out
0.000443	- out
0.000444	- out
0.000445	- out
0.000446	- out
0.000447	- out
0.000448	- out
0.000449	- out
0.00045	- out
0.000451	- out

	0.000452	- out						
	0.000453	- out						
	0.000454	- out						
	0.000455	- out						
	0.000456	- out						
	0.000457	- out						
	0.000458	- out						
	0.000459	- out						
151	0.00045916	7.7563e-005	275	79	275	3	30	0
	0.00046	- out						
	0.000461	- out						
	0.000462	- out						
	0.000463	- out						
	0.000464	- out						
	0.000465	- out						
	0.000466	- out						
	0.000467	- out						
	0.000468	- out						
	0.000469	- out						
	0.00047	- out						
	0.000471	- out						
	0.000472	- out						
	0.000473	- out						
	0.000474	- out						
	0.000475	- out						
	0.000476	- out						
	0.000477	- out						
	0.000478	- out						
152	0.00047855	1.9391e-005	279	80	279	2	31	0
	0.000479	- out						
	0.00048	- out						
	0.000481	- out						
	0.000482	- out						
	0.000483	- out						
	0.000484	- out						
	0.000485	- out						
	0.000486	- out						
	0.000487	- out						
	0.000488	- out						
153	0.00048825	9.6953e-006	282	82	282	2	32	0
	0.000489	- out						
	0.00049	- out						
	0.000491	- out						
	0.000492	- out						
	0.000493	- out						
154	0.00049309	4.8477e-006	285	84	285	2	33	0
	0.000494	- out						
	0.000495	- out						
155	0.00049552	2.4238e-006	288	86	288	2	34	0
	0.000496	- out						
156	0.00049673	1.2119e-006	291	88	291	2	35	0
	0.000497	- out						
	0.000498	- out						
	0.000499	- out						
157	0.00049915	2.4238e-006	292	89	292	2	35	0

158	0.00049946	3.0298e-007	297	92	297	2	37	0
159	0.00049961	1.5149e-007	300	94	300	2	38	0
160	0.00049991	3.0298e-007	301	95	301	2	38	0
161	0.00049995	3.7872e-008	306	98	306	2	40	0
162	0.00049997	1.8936e-008	309	100	309	2	41	0
163	0.00049998	9.4681e-009	312	102	312	2	42	0
164	0.0005	1.8936e-008	313	103	313	2	42	0
165	0.0005	2.367e-009	318	106	318	2	44	0
166	0.0005	2.9588e-010	323	109	323	2	46	0
167	0.0005	1.4794e-010	326	111	326	2	47	0
168	0.0005	7.3969e-011	329	113	329	2	48	0
169	0.0005	3.6985e-011	332	115	332	2	49	0
170	0.0005	1.8492e-011	335	117	335	2	50	0
171	0.0005	5.7789e-013	342	121	342	1	53	0
172	0.0005	2.8894e-013	345	123	345	1	54	0
173	0.0005	1.4447e-013	348	125	348	1	55	0
174	0.0005	7.2236e-014	352	127	352	1	56	0
175	0.0005	7.2236e-014	353	127	353	1	56	0
176	0.0005	6.5012e-014	355	127	355	1	56	0
177	0.0005	6.5012e-014	356	127	356	1	56	0
178	0.0005	6.5012e-014	357	127	357	1	56	0
179	0.0005	1.3002e-013	359	127	359	2	56	0
	0.0005	- out						
180	0.0005	1.3002e-013	360	127	360	2	56	0
181	0.0005	1.1076e-013	362	127	362	2	56	0
182	0.0005	1.1076e-013	363	127	363	2	56	0
183	0.0005	1.1076e-013	364	127	364	2	56	0
184	0.0005	1.1076e-013	365	127	365	2	56	0
185	0.0005	1.1076e-013	367	127	367	1	56	0
186	0.0005	1.1076e-013	368	127	368	1	56	0
187	0.0005	2.2152e-013	370	128	370	1	56	0
188	0.0005	2.2152e-013	371	128	371	1	56	0
189	0.0005	2.2152e-013	372	128	372	1	56	0
190	0.0005	4.4304e-013	374	128	374	2	56	0
191	0.0005	4.4304e-013	375	128	375	2	56	0
192	0.0005	8.8608e-013	377	129	377	2	56	0
193	0.0005	8.8608e-013	378	129	378	2	56	0
194	0.0005	8.8608e-013	379	129	379	2	56	0
195	0.0005	8.8608e-013	380	129	380	2	56	0
196	0.0005	1.7722e-012	382	129	382	3	56	0
197	0.0005	1.7722e-012	383	129	383	3	56	0
198	0.0005	3.5443e-012	385	130	385	3	56	0
199	0.0005	3.0655e-012	387	130	387	3	56	0
200	0.0005	3.0655e-012	388	130	388	3	56	0
201	0.0005	3.0655e-012	389	130	389	3	56	0
202	0.0005	3.0655e-012	390	130	390	3	56	0
203	0.0005	3.0655e-012	391	130	391	3	56	0
204	0.0005	3.0655e-012	392	130	392	3	56	0
205	0.0005	4.4546e-012	396	130	396	4	57	0
206	0.0005	4.4546e-012	397	130	397	4	57	0
207	0.0005	4.4546e-012	398	130	398	4	57	0
208	0.0005	4.4546e-012	399	130	399	4	57	0
209	0.0005	4.4546e-012	400	130	400	4	57	0
210	0.0005	4.4546e-012	401	130	401	4	57	0
211	0.0005	4.4546e-012	402	130	402	4	57	0

212	0.0005	8.0184e-012	406	131	406	3	58	0
213	0.0005	8.0184e-012	407	131	407	3	58	0
214	0.0005	8.0184e-012	408	131	408	3	58	0
215	0.0005	8.0184e-012	409	131	409	3	58	0
216	0.0005	8.0184e-012	410	131	410	3	58	0
217	0.0005	8.0184e-012	411	131	411	3	58	0
218	0.0005	1.6037e-011	413	132	413	3	58	0
219	0.0005	1.6037e-011	415	132	415	2	58	0
220	0.0005	1.6037e-011	416	132	416	2	58	0
221	0.0005	3.2073e-011	418	133	418	2	58	0
222	0.0005	3.2073e-011	419	133	419	2	58	0
223	0.0005	6.4147e-011	421	134	421	2	58	0
224	0.0005	6.4147e-011	422	134	422	2	58	0
225	0.0005	6.4147e-011	423	134	423	2	58	0
226	0.0005	6.4147e-011	424	134	424	2	58	0
227	0.0005	1.2829e-010	426	135	426	1	58	0
228	0.0005	2.5659e-010	428	136	428	1	58	0
229	0.0005	5.1318e-010	429	137	429	1	58	0
230	0.0005	1.0264e-009	430	138	430	1	58	0
231	0.0005	2.0527e-009	431	139	431	1	58	0
232	0.00050001	4.1054e-009	432	140	432	1	58	0
233	0.00050002	8.2108e-009	433	141	433	1	58	0
234	0.00050003	1.6422e-008	434	142	434	1	58	0
235	0.00050007	3.2843e-008	435	143	435	1	58	0
236	0.00050013	6.5686e-008	436	144	436	1	58	0
237	0.00050026	1.3137e-007	437	145	437	1	58	0
238	0.00050053	2.6275e-007	439	146	439	1	58	0
	0.000501	- out						
239	0.00050105	5.2549e-007	441	147	441	1	58	0
240	0.00050158	5.2549e-007	442	147	442	1	58	0
	0.000502	- out						
241	0.00050263	1.051e-006	444	148	444	1	58	0
	0.000503	- out						
242	0.00050357	9.4589e-007	446	148	446	1	58	0
	0.000504	- out						
243	0.00050452	9.4589e-007	447	148	447	1	58	0
	0.000505	- out						
244	0.00050547	9.4589e-007	448	148	448	1	58	0
	0.000506	- out						
	0.000507	- out						
245	0.00050736	1.8918e-006	450	148	450	2	58	0
	0.000508	- out						
	0.000509	- out						
246	0.00050925	1.8918e-006	451	148	451	2	58	0
	0.00051	- out						
	0.000511	- out						
247	0.00051114	1.8918e-006	452	148	452	2	58	0
	0.000512	- out						
	0.000513	- out						
	0.000514	- out						
248	0.00051492	3.7835e-006	454	149	454	2	58	0
	0.000515	- out						
	0.000516	- out						
	0.000517	- out						
	0.000518	- out						

249	0.00051815	3.2233e-006	456	149	456	2	58	0
	0.000519	- out						
	0.00052	- out						
	0.000521	- out						
250	0.00052137	3.2233e-006	457	149	457	2	58	0
	0.000522	- out						
	0.000523	- out						
	0.000524	- out						
251	0.00052459	3.2233e-006	458	149	458	2	58	0
	0.000525	- out						
	0.000526	- out						
	0.000527	- out						
252	0.00052782	3.2233e-006	459	149	459	2	58	0
	0.000528	- out						
	0.000529	- out						
	0.00053	- out						
	0.000531	- out						
253	0.00053104	3.2233e-006	461	149	461	3	58	0
	0.000532	- out						
	0.000533	- out						
	0.000534	- out						
254	0.00053426	3.2233e-006	462	149	462	3	58	0
	0.000535	- out						
	0.000536	- out						
	0.000537	- out						
	0.000538	- out						
	0.000539	- out						
	0.00054	- out						
255	0.00054071	6.4465e-006	464	149	464	3	58	0
	0.000541	- out						
	0.000542	- out						
	0.000543	- out						
	0.000544	- out						
	0.000545	- out						
	0.000546	- out						
256	0.00054651	5.8019e-006	466	149	466	3	58	0
	0.000547	- out						
	0.000548	- out						
	0.000549	- out						
	0.00055	- out						
	0.000551	- out						
	0.000552	- out						
257	0.00055231	5.8019e-006	467	149	467	3	58	0
	0.000553	- out						
	0.000554	- out						
	0.000555	- out						
	0.000556	- out						
	0.000557	- out						
	0.000558	- out						
258	0.00055812	5.8019e-006	468	149	468	3	58	0
	0.000559	- out						
	0.00056	- out						
	0.000561	- out						
	0.000562	- out						
	0.000563	- out						

259	0.00056392	5.8019e-006	469	149	469	3	58	0
	0.000564	- out						
	0.000565	- out						
	0.000566	- out						
	0.000567	- out						
	0.000568	- out						
	0.000569	- out						
260	0.00056972	5.8019e-006	470	149	470	3	58	0
	0.00057	- out						
	0.000571	- out						
	0.000572	- out						
	0.000573	- out						
	0.000574	- out						
	0.000575	- out						
261	0.00057552	5.8019e-006	471	149	471	3	58	0
	0.000576	- out						
	0.000577	- out						
	0.000578	- out						
	0.000579	- out						
	0.00058	- out						
	0.000581	- out						
262	0.00058132	5.8019e-006	473	149	473	4	58	0
	0.000582	- out						
	0.000583	- out						
	0.000584	- out						
	0.000585	- out						
	0.000586	- out						
	0.000587	- out						
263	0.00058713	5.8019e-006	474	149	474	4	58	0
	0.000588	- out						
	0.000589	- out						
	0.00059	- out						
	0.000591	- out						
	0.000592	- out						
264	0.00059293	5.8019e-006	475	149	475	4	58	0
	0.000593	- out						
	0.000594	- out						
	0.000595	- out						
	0.000596	- out						
	0.000597	- out						
	0.000598	- out						
265	0.00059873	5.8019e-006	476	149	476	4	58	0
	0.000599	- out						
	0.0006	- out						
	0.000601	- out						
	0.000602	- out						
	0.000603	- out						
	0.000604	- out						
266	0.00060453	5.8019e-006	477	149	477	4	58	0
	0.000605	- out						
	0.000606	- out						
	0.000607	- out						
	0.000608	- out						
	0.000609	- out						
	0.00061	- out						

267	0.00061033	5.8019e-006	478	149	478	4	58	0
	0.000611	- out						
	0.000612	- out						
	0.000613	- out						
	0.000614	- out						
	0.000615	- out						
	0.000616	- out						
268	0.00061613	5.8019e-006	479	149	479	4	58	0
	0.000617	- out						
	0.000618	- out						
	0.000619	- out						
	0.00062	- out						
	0.000621	- out						
269	0.00062194	5.8019e-006	481	149	481	5	58	0
	0.000622	- out						
	0.000623	- out						
	0.000624	- out						
	0.000625	- out						
	0.000626	- out						
	0.000627	- out						
	0.000628	- out						
	0.000629	- out						
	0.00063	- out						
	0.000631	- out						
	0.000632	- out						
	0.000633	- out						
270	0.00063354	1.1604e-005	483	150	483	4	58	0
	0.000634	- out						
	0.000635	- out						
	0.000636	- out						
	0.000637	- out						
	0.000638	- out						
	0.000639	- out						
	0.00064	- out						
	0.000641	- out						
	0.000642	- out						
	0.000643	- out						
271	0.00064398	1.0443e-005	485	150	485	4	58	0
	0.000644	- out						
	0.000645	- out						
	0.000646	- out						
	0.000647	- out						
	0.000648	- out						
	0.000649	- out						
	0.00065	- out						
	0.000651	- out						
	0.000652	- out						
	0.000653	- out						
	0.000654	- out						
272	0.00065443	1.0443e-005	486	150	486	4	58	0
	0.000655	- out						
	0.000656	- out						
	0.000657	- out						
	0.000658	- out						
	0.000659	- out						

	0.00066	- out						
	0.000661	- out						
	0.000662	- out						
	0.000663	- out						
	0.000664	- out						
273	0.00066487	1.0443e-005	487	150	487	4	58	0
	0.000665	- out						
	0.000666	- out						
	0.000667	- out						
	0.000668	- out						
	0.000669	- out						
	0.00067	- out						
	0.000671	- out						
	0.000672	- out						
	0.000673	- out						
	0.000674	- out						
	0.000675	- out						
274	0.00067531	1.0443e-005	488	150	488	4	58	0
	0.000676	- out						
	0.000677	- out						
	0.000678	- out						
	0.000679	- out						
	0.00068	- out						
	0.000681	- out						
	0.000682	- out						
	0.000683	- out						
	0.000684	- out						
	0.000685	- out						
275	0.00068576	1.0443e-005	489	150	489	4	58	0
	0.000686	- out						
	0.000687	- out						
	0.000688	- out						
	0.000689	- out						
	0.00069	- out						
	0.000691	- out						
	0.000692	- out						
	0.000693	- out						
	0.000694	- out						
	0.000695	- out						
	0.000696	- out						
276	0.0006962	1.0443e-005	490	150	490	4	58	0
	0.000697	- out						
	0.000698	- out						
	0.000699	- out						
	0.0007	- out						
	0.000701	- out						
	0.000702	- out						
	0.000703	- out						
	0.000704	- out						
	0.000705	- out						
	0.000706	- out						
277	0.00070664	1.0443e-005	491	150	491	4	58	0
	0.000707	- out						
	0.000708	- out						
	0.000709	- out						

	0.00071	- out						
	0.000711	- out						
	0.000712	- out						
	0.000713	- out						
	0.000714	- out						
	0.000715	- out						
	0.000716	- out						
	0.000717	- out						
278	0.00071709	1.0443e-005	492	150	492	4	58	0
	0.000718	- out						
	0.000719	- out						
	0.00072	- out						
	0.000721	- out						
	0.000722	- out						
	0.000723	- out						
	0.000724	- out						
	0.000725	- out						
	0.000726	- out						
	0.000727	- out						
279	0.00072753	1.0443e-005	494	150	494	5	58	0
	0.000728	- out						
	0.000729	- out						
	0.00073	- out						
	0.000731	- out						
	0.000732	- out						
	0.000733	- out						
	0.000734	- out						
	0.000735	- out						
	0.000736	- out						
	0.000737	- out						
280	0.00073797	1.0443e-005	495	150	495	5	58	0
	0.000738	- out						
	0.000739	- out						
	0.00074	- out						
	0.000741	- out						
	0.000742	- out						
	0.000743	- out						
	0.000744	- out						
	0.000745	- out						
	0.000746	- out						
	0.000747	- out						
	0.000748	- out						
281	0.00074842	1.0443e-005	496	150	496	5	58	0
	0.000749	- out						
	0.00075	- out						
	0.000751	- out						
	0.000752	- out						
	0.000753	- out						
	0.000754	- out						
	0.000755	- out						
	0.000756	- out						
	0.000757	- out						
	0.000758	- out						
282	0.00075886	1.0443e-005	497	150	497	5	58	0
	0.000759	- out						

	0.00076	- out						
	0.000761	- out						
	0.000762	- out						
	0.000763	- out						
	0.000764	- out						
	0.000765	- out						
	0.000766	- out						
	0.000767	- out						
	0.000768	- out						
	0.000769	- out						
283	0.0007693	1.0443e-005	498	150	498	5	58	0
	0.00077	- out						
	0.000771	- out						
	0.000772	- out						
	0.000773	- out						
	0.000774	- out						
	0.000775	- out						
	0.000776	- out						
	0.000777	- out						
	0.000778	- out						
	0.000779	- out						
284	0.00077975	1.0443e-005	499	150	499	5	58	0
	0.00078	- out						
	0.000781	- out						
	0.000782	- out						
	0.000783	- out						
	0.000784	- out						
	0.000785	- out						
	0.000786	- out						
	0.000787	- out						
	0.000788	- out						
	0.000789	- out						
	0.00079	- out						
285	0.00079019	1.0443e-005	501	150	501	4	58	0
	0.000791	- out						
	0.000792	- out						
	0.000793	- out						
	0.000794	- out						
	0.000795	- out						
	0.000796	- out						
	0.000797	- out						
	0.000798	- out						
	0.000799	- out						
	0.0008	- out						
286	0.00080063	1.0443e-005	502	150	502	4	58	0
	0.000801	- out						
	0.000802	- out						
	0.000803	- out						
	0.000804	- out						
	0.000805	- out						
	0.000806	- out						
	0.000807	- out						
	0.000808	- out						
	0.000809	- out						
	0.00081	- out						

	0.000811	- out						
287	0.00081108	1.0443e-005	503	150	503	4	58	0
	0.000812	- out						
	0.000813	- out						
	0.000814	- out						
	0.000815	- out						
	0.000816	- out						
	0.000817	- out						
	0.000818	- out						
	0.000819	- out						
	0.00082	- out						
	0.000821	- out						
	0.000822	- out						
	0.000823	- out						
	0.000824	- out						
	0.000825	- out						
	0.000826	- out						
288	0.00082653	1.5455e-005	507	151	507	4	59	0
	0.000827	- out						
	0.000828	- out						
	0.000829	- out						
	0.00083	- out						
	0.000831	- out						
	0.000832	- out						
	0.000833	- out						
	0.000834	- out						
	0.000835	- out						
	0.000836	- out						
	0.000837	- out						
	0.000838	- out						
	0.000839	- out						
	0.00084	- out						
	0.000841	- out						
289	0.00084199	1.5455e-005	508	151	508	4	59	0
	0.000842	- out						
	0.000843	- out						
	0.000844	- out						
	0.000845	- out						
	0.000846	- out						
	0.000847	- out						
	0.000848	- out						
	0.000849	- out						
	0.00085	- out						
	0.000851	- out						
	0.000852	- out						
	0.000853	- out						
	0.000854	- out						
	0.000855	- out						
	0.000856	- out						
	0.000857	- out						
290	0.00085744	1.5455e-005	509	151	509	4	59	0
	0.000858	- out						
	0.000859	- out						
	0.00086	- out						
	0.000861	- out						

	0.000862	- out						
	0.000863	- out						
	0.000864	- out						
	0.000865	- out						
	0.000866	- out						
	0.000867	- out						
	0.000868	- out						
	0.000869	- out						
	0.00087	- out						
	0.000871	- out						
	0.000872	- out						
291	0.0008729	1.5455e-005	511	151	511	4	59	0
	0.000873	- out						
	0.000874	- out						
	0.000875	- out						
	0.000876	- out						
	0.000877	- out						
	0.000878	- out						
	0.000879	- out						
	0.00088	- out						
	0.000881	- out						
	0.000882	- out						
	0.000883	- out						
	0.000884	- out						
	0.000885	- out						
	0.000886	- out						
	0.000887	- out						
	0.000888	- out						
292	0.00088835	1.5455e-005	513	151	513	4	59	0
	0.000889	- out						
	0.00089	- out						
	0.000891	- out						
	0.000892	- out						
	0.000893	- out						
	0.000894	- out						
	0.000895	- out						
	0.000896	- out						
	0.000897	- out						
	0.000898	- out						
	0.000899	- out						
	0.0009	- out						
	0.000901	- out						
	0.000902	- out						
	0.000903	- out						
293	0.00090381	1.5455e-005	515	151	515	4	59	0
	0.000904	- out						
	0.000905	- out						
	0.000906	- out						
	0.000907	- out						
	0.000908	- out						
	0.000909	- out						
	0.00091	- out						
	0.000911	- out						
	0.000912	- out						
	0.000913	- out						

	0.000914	- out						
	0.000915	- out						
	0.000916	- out						
	0.000917	- out						
	0.000918	- out						
	0.000919	- out						
294	0.00091926	1.5455e-005	517	151	517	5	59	0
	0.00092	- out						
	0.000921	- out						
	0.000922	- out						
	0.000923	- out						
	0.000924	- out						
	0.000925	- out						
	0.000926	- out						
	0.000927	- out						
	0.000928	- out						
	0.000929	- out						
	0.00093	- out						
	0.000931	- out						
	0.000932	- out						
	0.000933	- out						
	0.000934	- out						
295	0.00093472	1.5455e-005	519	151	519	5	59	0
	0.000935	- out						
	0.000936	- out						
	0.000937	- out						
	0.000938	- out						
	0.000939	- out						
	0.00094	- out						
	0.000941	- out						
	0.000942	- out						
	0.000943	- out						
	0.000944	- out						
	0.000945	- out						
	0.000946	- out						
	0.000947	- out						
	0.000948	- out						
	0.000949	- out						
	0.00095	- out						
296	0.00095018	1.5455e-005	522	151	522	5	59	0
	0.000951	- out						
	0.000952	- out						
	0.000953	- out						
	0.000954	- out						
	0.000955	- out						
	0.000956	- out						
	0.000957	- out						
	0.000958	- out						
	0.000959	- out						
	0.00096	- out						
	0.000961	- out						
	0.000962	- out						
	0.000963	- out						
	0.000964	- out						
	0.000965	- out						

297	0.00096563	1.5455e-005	524	151	524	5	59	0
	0.000966	- out						
	0.000967	- out						
	0.000968	- out						
	0.000969	- out						
	0.00097	- out						
	0.000971	- out						
	0.000972	- out						
	0.000973	- out						
	0.000974	- out						
	0.000975	- out						
	0.000976	- out						
	0.000977	- out						
	0.000978	- out						
	0.000979	- out						
	0.00098	- out						
	0.000981	- out						
298	0.00098109	1.5455e-005	526	151	526	5	59	0
	0.000982	- out						
	0.000983	- out						
	0.000984	- out						
	0.000985	- out						
	0.000986	- out						
	0.000987	- out						
	0.000988	- out						
	0.000989	- out						
	0.00099	- out						
	0.000991	- out						
	0.000992	- out						
	0.000993	- out						
	0.000994	- out						
	0.000995	- out						
	0.000996	- out						
299	0.00099654	1.5455e-005	529	151	529	5	59	0
	0.000997	- out						
	0.000998	- out						
	0.000999	- out						
	0.001	- out						
300	0.001012	1.5455e-005	531	151	531	4	59	0

Time-stepping completed.

Time-

Dependent Solver 1 in Solver 1: Solution time: 253 s. (4 minutes, 13 seconds)

Fully Coupled 1 (fc1)